

LCFELMV2
Low Carbon Footprint Electric Lawn Mower
Version 2

Final Report

Jeff Garza
Jason Gualandi
Dustin Hohenbery

Advisors:
Dr. Huggins
Mr. Gutschlag

May 14, 2009

Abstract

The goal of this project is to design a low carbon footprint lawn mower using a battery-powered electric motor and photovoltaic battery charging system. The mower platform with batteries will perform at the level of a high-end gas powered lawn mower with similar weight. An appropriate sized brushed DC motor was purchased, tested and then modeled in Simulink. The Simulink model was used to help determine the margin of operation under heavy loads (i.e. long grass) and power consumption. Optimal capacity batteries were also purchased and integrated with the motor and a display. The charging system was constrained by cost of the PV array versus charging time and dependence on AC utility power. Initially the price of the system will be higher than a gas powered lawn mower, but cost trends could be identified in the critical technologies which will ultimately lead to competitive pricing of the system relative to high end gas powered lawn mowers.

Table of Contents

Abstract.....	ii
Table of Contents.....	iii
Table of Equations.....	v
Table of Figures.....	v
Introduction.....	1
I. Project Summary.....	1
II. Functional Description and Requirements.....	1
A. Functional Description of Mower System.....	1
B. Block Diagram of Mower System and Functional Requirements of Subsystem Components.....	2
C. Functional Description of Charger System.....	3
D. Block Diagram of Charger System and Functional Requirements of Subsystem Components.....	4
E. Software Flow Chart for Control of Charger System.....	5
1. Charging Module Flow Chart.....	6
2. Stop Module Flow Chart.....	7
III. Design Considerations.....	8
A. Motor.....	8
1. Permanent Magnet (PM) DC Motor Characteristics.....	9
a. Measurement of R_a and L_a	9
b. Measurement of Motor Constant, K_e and K_t	10
c. Measurement of $T_{S.F.}$ and b	11
d. Measurement of J	11
e. Motor Characteristics Values.....	12
2. PM DC Motor Simulink Model.....	13
B. Mower System.....	14
1. Safety Considerations.....	14
a. Manual On/Off Safety Switch.....	14
b. Pull Bar Safety Switch.....	15
2. Mower System Simulation.....	16
a. Measurement of J_b	17
b. Measurement of T_{spin}	18
b. Measurement of $T_{cutting}$	18
3. Field Test Data Collection.....	18
4. Cutting Power Calculation.....	20
C. Battery.....	21
D. PV Charging.....	22
E. Charging System Implementation.....	23
1. Charging System Wiring Diagram.....	23
2. Current Sensor Testing.....	25

3. Relay Testing	26
4. Combined Component Testing Without Current Sensor	27
5. Complete Charging System Testing	27
IV. Results	28
V. Recommendations for Future Work	29
VI. Parts List	29
VII. Patents	30
VIII. Standards	34
A. PV Standards	34
B. ATSM Standards	35
C. PVGAP Standards	35
D. ISO Standards	35
E. UL Standards	35
F. Motor Standards	36
G. Power Standards	36
H. General Appliance Standards	36
I. IEC Standards	36
References	38
Appendix	39
Motor Scott Performance Curves	39
NPC-4200 Performance Curves	40
Isolation Data – June	41
Isolation Data – May	42
Isolation Data – September	43

Table of Equations

Equation 1 - Armature Resistance Calculation.....	9
Equation 2 - Equation to Calculate L_a	10
Equation 3 - Equation for Motor Constants.....	11
Equation 4 – Sum of All Torques.....	11
Equation 5 – Summation of All Torques during Coast-Down.....	12
Equation 6 – Mass Moment of Inertia.....	12
Equation 7 – Mass Moment of Inertia for Solid Cylinder with Central Axis of Cylinder.....	18
Equation 8 – Mass Moment of Inertia for Rectangular Plate with Axis through Center..	18
Equation 9 – Required Battery Capacity.....	21
Equation 10 – PV output (J/day).....	22
Equation 11 – PV System, days needed to charge battery.....	22
Equation 12 – Days needed to charge battery for 4kWh/m ² /day radiation.....	23

Table of Figures

Figure 1 – Mower System Block Diagram.....	1
Figure 2 - Lawn Mower Block Diagram.....	2
Figure 3 – Charger System Block Diagram.....	3
Figure 4 - Battery Charger Block Diagram.....	4
Figure 5 – Charger Controller Flow Chart.....	6
Figure 6 – Charger Controller Stop Module Flow Chart.....	7
Figure 7 - Simulink PM DC Motor Model.....	9
Figure 8 - Circuit to find R_a and L_a	10
Figure 9 – Ramp Up Current for Locked Rotor Test.....	10
Figure 10 - Circuit Used for Motor Testing.....	11
Figure 11 - Results of Coast-Down Test.....	12
Figure 12 - Simulink Model for PM DC Motor.....	13
Figure 13 - Graph of Simulink vs. Experimental for Motor Only.....	14
Figure 14 – Time Delay Values for Carlington Breakers.....	15
Figure 15 – Pull Bar Safety Switch for Motor Starting.....	16
Figure 16 - Mower System Simulation.....	17
Figure 17 - Force Terms for Simulation.....	17
Figure 18 – Charging System Wiring Diagram.....	24
Figure 19 - Current Sensor Testing Diagram.....	25
Figure 20 – Graph for Current Sensor Output.....	26
Figure 21 - Relay Testing Diagram.....	27
Figure 22 - System Testing Diagram.....	27
Figure 23 – Motor Scott 1 HP performance curves at 24 volts.....	39
Figure 24 – NPC-4200 performance curves based on dyno test data.....	40
Figure 25 – Isolation Data for June, Minimum Daily Solar Radiation.....	41
Figure 26 – Isolation Data for May, Minimum Daily Solar Radiation.....	42
Figure 27 – Isolation Data for September, Minimum Daily Solar Radiation.....	43

Introduction

This report discusses the redesign of the Low Carbon Footprint Electric Lawn Mower (LCFELM) originally done as a senior project in 2007-08. This first system used lead acid batteries and an inefficient DC motor. It was low cost but very heavy. Furthermore, the Photo Voltaic (PV) charging system was not implemented. The LCFELMv2 project in 2008-09 took on the challenge of redesigning the mower with the goal of dramatically decreasing the weight of the system while maintaining functionality. In addition, the charging system was functional and optimized using “off the shelf” electronics and minimal extra components.

I. Project Summary

The goal of this project was to design a low carbon footprint lawn mower using a battery powered electric motor and photovoltaic battery charging system. The prototype would perform at the level of a high-end gas powered lawn mower with similar weight. Initially the price would be higher than a gas powered lawn mower, but cost trends could be identified in the critical technologies which would ultimately lead to competitive pricing of the LCFELMV2.

II. Functional Description and Requirements

This section discusses the functional descriptions and requirements for the project and covers the mower and the charging systems.

A. Functional Description of Mower System

The electric motor will have sufficient power and torque to rotate the cutting blade in normal operation. It will also be implemented with electronics and a hold down a safety switch on the handle so the cutting blade will stop rotating in 3 seconds when user releases the switch.



Figure 1 – Mower System Block Diagram

Mower System Requirements

Mowing Capability: The lawn mower shall be able to mow a 10,000 ft² area or operate for at least one hour when operation begins with a fully charged battery array.

Safety Features: The mower shall have a safety switch on the handle which will need to be held down for the mower to start spinning the blade. Other safety regulations required by law shall be included as well.

Weight: The weight of the mower shall not exceed 65 lbs.

Deck Size: The size of the deck and blade shall yield a 19 inch cutting swath.

B. Block Diagram of Mower System and Functional Requirements of Subsystem Components

The lawn mower block diagram is shown in Figure 2. It displays the overall mower system and the power and data signals.

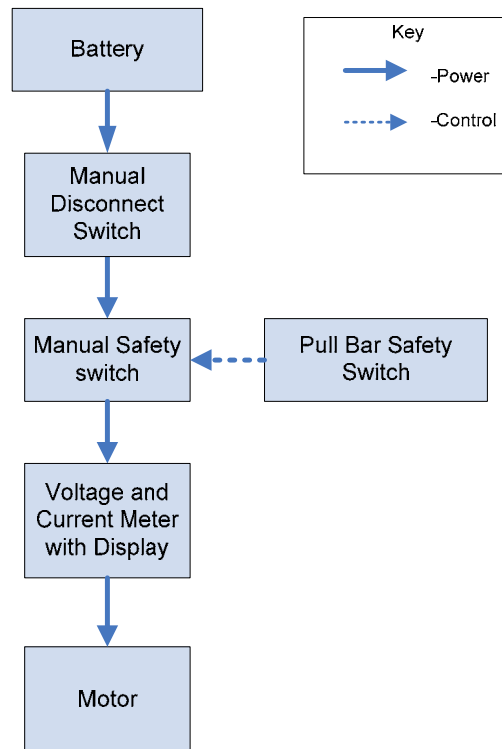


Figure 2 - Lawn Mower Block Diagram

Lawn Mower Subsystem Requirements

Battery: A battery with sufficient amp hours shall be chosen to run the system for at least one hour and/or mow a 10,000 ft² lawn. Two 12V deep discharge sealed lead acid batteries shall be connected in series to provide 24V.

Manual Safety Switch: A switch shall be used to turn the mower electrical system on and off. When the switch is off, no power shall be supplied to the display electronics or manual safety switch. When the switch is on, power shall be supplied to the display electronics and the manual safety switch.

Manual Safety Switch: When the user releases the manual safety switch the system shall power down and cutting blade stop rotating in 3 seconds or less.

Display: The display shall consist of a 2 line LCD display. This display shall show the voltage to the system and the current drawn by the motor

Motor: The mower shall use a 24V DC brushed motor that obtains peak efficiency at 3300 RPM.

C. Functional Description of Charger System

The charging system will use primarily solar energy, with AC grid power as a back up, to charge the mower's batteries. The charging system shall switch from solar energy to AC power when needed to charge the batteries in a timely manner. The charging system will be implemented using off the shelf components.

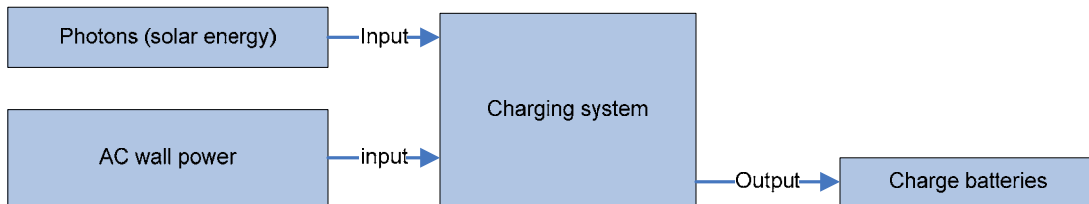


Figure 3 – Charger System Block Diagram

Charger System Requirements

Duration of Charge: The batteries shall be fully charged in no more than 4 days. The microcontroller will utilize solar power while only using AC power when necessary.

Easy Interface: The batteries shall have power connections that can be connected to the charger safely. An on off switch shall be used to allow for safe and easy battery connection.

Charger Controller: Charger controller shall be compatible with the battery chemistry and charge the batteries at a safe rate and in a fashion to maximize battery cycle life.

D. Block Diagram of Charger System and Functional Requirements of Subsystem Components

The block diagram of the charger system is shown in Figure 4. Solar power and AC power are utilized in complementary fashion to charge the battery in a timely manner depending on the solar power output of the PV array. The interconnection of the subsystem components is shown with power and control signals.

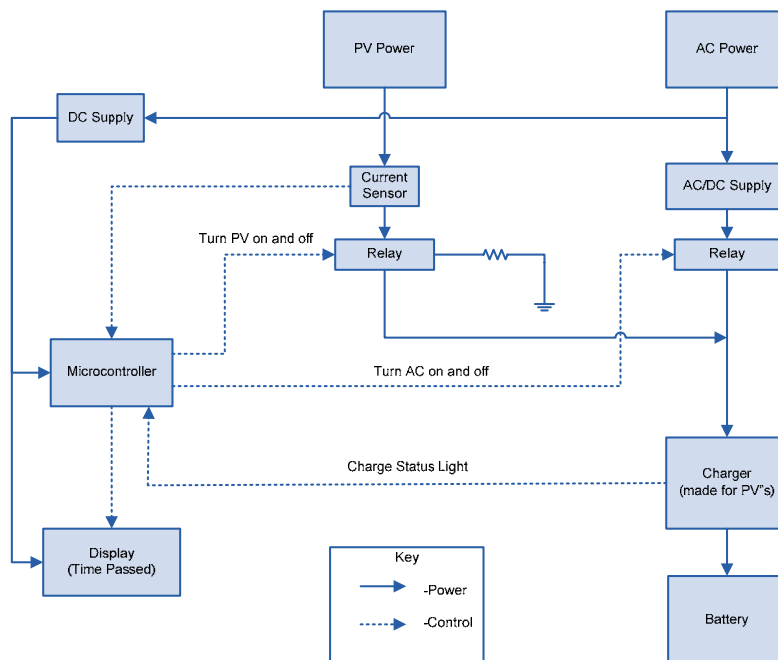


Figure 4 - Battery Charger Block Diagram

Charger Subsystem Requirements

AC Power: The charger system shall use standard household AC power.

Relays: The electromechanical relays shall switch the power supply between AC power and solar power to charge the batteries. The relays shall be controlled by the microcontroller. The relays will handle up to 5 amps. The control input resistance will be less than 100mΩ.

DC Supply: The DC supply shall take AC power and convert it to DC voltage and current levels similar to the solar panel DC voltage and current levels at maximum output.

Current Sensor: The current sensor shall measure current from 0 to 3 Amps and output an analog signal to the controller. The current sensor shall have 1% accuracy.

Solar Power and Photo Voltaic (PV) Array: The PV array shall have the capacity to charge the battery in 3 days during peak growing period during the summer month of June, and charge the battery in 7 days in the month of September. The location being used for the design is the Midwest, and a large enough surface area shall be needed to charge two 12 volt batteries in four days. The angle of the solar panel shall be determined by the demographic location of the mower in the Midwest. The voltage supplied at the maximum power shall be 17.5Vdc, and the current supplied at the maximum power shall be 2.9A. The PV array is the same array used by the 2007-2008 team.

Microcontroller: The microcontroller shall take current sensor inputs to determine whether to use solar power or backup power. The design shall be optimized to fully charge the batteries to full capacity in 4 days.

Charger: The charger shall be an off the shelf component compatible with the sealed lead acid batteries and be powered by the solar panel. The charger shall have charge status output signals.

E. Software Flow Chart for Control of Charger System

The charging system controls the automatic selection of Solar Power or AC Power as needed. The system uses AC Power only as needed after three days has passed. The charging module and stop module are the main components for the charging system.

1. Charging Module Flow Chart

The software flow chart for the microcontroller is displayed in Figure 5. The program shall control the automatic selection of AC Power or Solar Power as needed. The system uses AC Power only as needed only after three days has passed.

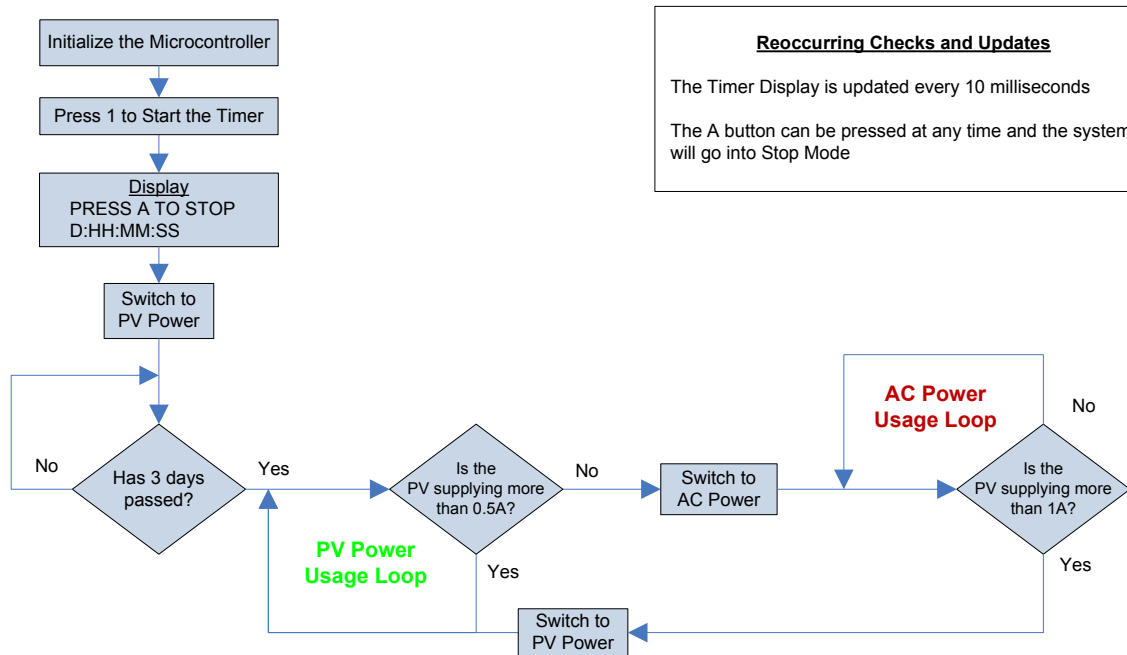


Figure 5 – Charger Controller Flow Chart

Charging Module Characteristics

Prompt to Start: The system asks the user to “PRESS 1 TO START THE TIMER”. Once the user presses “1” the system starts the timer.

Display: The timer loop increments the clock in 10 millisecond increments. Until the user presses “A” the system is fully automated. If “A” is pressed the system goes to the stop module.

Three Day Loop: Once the system is started the clock counts the time that has passed since the user pressed “1”. After three days has passed the system goes into the PV Power Usage Loop.

Power Usage Loop: In the PV Power Usage Loop the system checks the current available from the PV array. If the current drops below .5amps the systems switches to AC and goes into the AC Power Usage Loop.

AC Power Usage Loop: In the AC Power Usage Loop the system checks the current available from the PV array. If the current raises above 1amp the system switches to PV Power and returns to the PV Power Usage Loop.

2. Stop Module Flow Chart

The stop module for the charging system is displayed in Figure 6 below. When the user presses “A” at anytime during operation the system will go to the stop module.

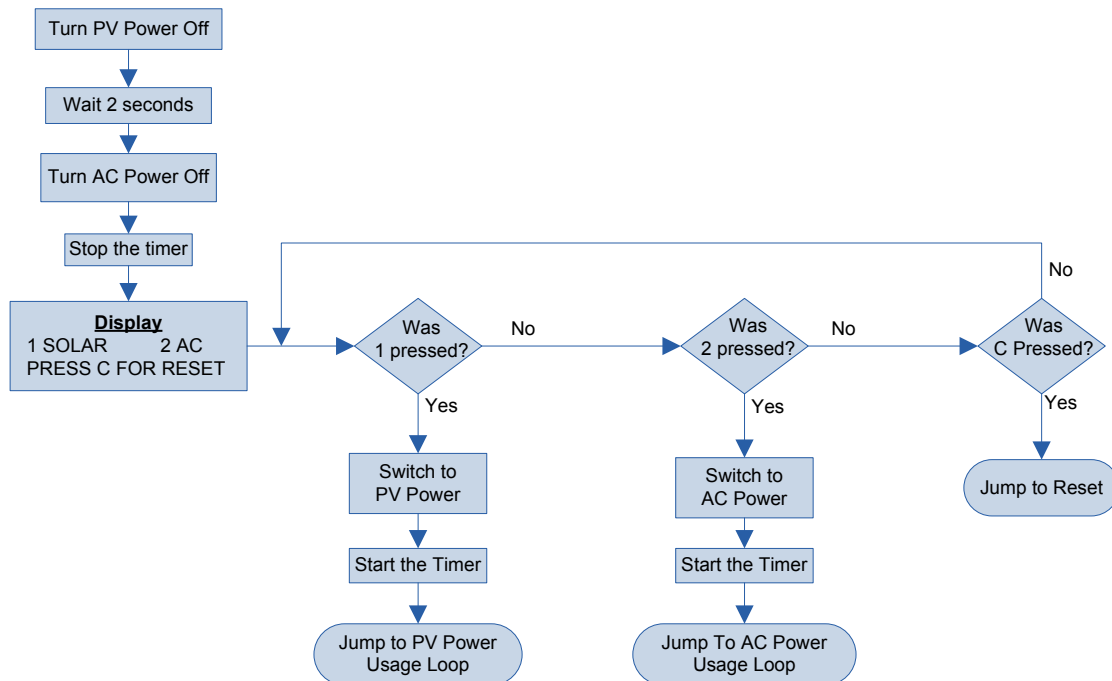


Figure 6 – Charger Controller Stop Module Flow Chart

Stop Module Characteristics

Display: After reaching the stop module the system switches to an off condition. This ensures no current flow through the charger controller. The system will display “1 Solar 2 AC” on the first line of the display and “PRESS C FOR RESET” on the second line of the display.

Loop: The system will loop until the user presses “1”, “2”, or “C”. When “1” is pressed the system switches to PV Power and goes to the PV Power Usage Loop. When “2” is pressed the system switches to AC Power and goes to the AC Power Usage Loop. When “C” is pressed the system resets goes to the Prompt To Start.

III. Design Considerations

This section discusses the major design considerations for the project and covers the motor, batteries, and the charging system.

A. Motor

A main goal of the redesign is decrease the weight of the mower. Thus, the team focused on finding a motor that was more efficient and lighter weight. In order to specify the size of the motor, the team needed to determine the cutting power required to cut grass at different stages of growth and ground cover. This was done by using the field test data from last year’s project. Though an efficiency value was not available for the motor used in 2007-08, it was assumed that the motor specified for version 2 would be about 20% more efficient. Thus, it is reasonable to use the field test data to give a worst case estimate of the power needed for version 2, shown in Table 1.

Table 1 – Field Test 2007, tested by Kraig Kamp, David Sharpe, and Jamin Williams¹

Field Test		Outside Conditions: Partly Cloudy Relatively Dry, 40°F, 11/29/2007 2:15:00 PM		
Sample	<u>Mowing Conditions</u>	Current (A)	Voltage (V)	Watts (W)
1	Lowest blade height, high grass density, full leaf coverage, standing still	13	22.5	292.5
2	Lowest blade height, high grass density, full leaf coverage, walking	25	22.0	550.0
3	Lowest blade height, high grass density, full leaf coverage, bogged down	35	20.0	700.0
4	Highest blade height, high grass density, full leaf coverage, walking	20	21.2	424.0
5	Lowest blade height, average grass density, no leaves, standing still	14	22.2	310.8
6	Lowest blade height, average grass density, no leaves, walking	16	21.7	347.2
7	Lowest blade height, high grass density, no leaves, walking	19	21.0	399.0
8	On concrete, standing still	11	21.3	234.3
Average running current		19.1	21.5	410.9

Several motors were identified that could supply the worst case estimated power needed. The final choice, the Scott Motor 1+ HP "Electrathon" (see http://www.beepscom.com/product_p/mo-4bb3995.htm following), was based on weight, operating voltage, power-rpm characteristic, efficiency, cost and availability. This motor operates at 24 volts, weighs 14.1 lbs, and has peak efficiency at 2800 RPM.

¹ Kamp, Kraig, David Sharpe, and Jamin Williams. Low Carbon Footprint Electric Lawn Mower. Electrical Engineering, Bradley University.

1. Permanent Magnet (PM) DC Motor Characteristics

Once the motor was selected the team developed an accurate motor model and used Simulink to run simulations. Unfortunately, the motor did not have a data sheet and the team had to test the motor in order to obtain the following parameters: armature resistance (R_a), armature inductance (L_a), torque constant (K_t), electrical constant, mass moment of inertia (J), viscous friction (b), and static friction (T_{SF}). The experimental techniques used to find these parameters are discussed in the following subsections. Once found, the parameter values were then put into the Simulink block diagram shown in Figure 7.

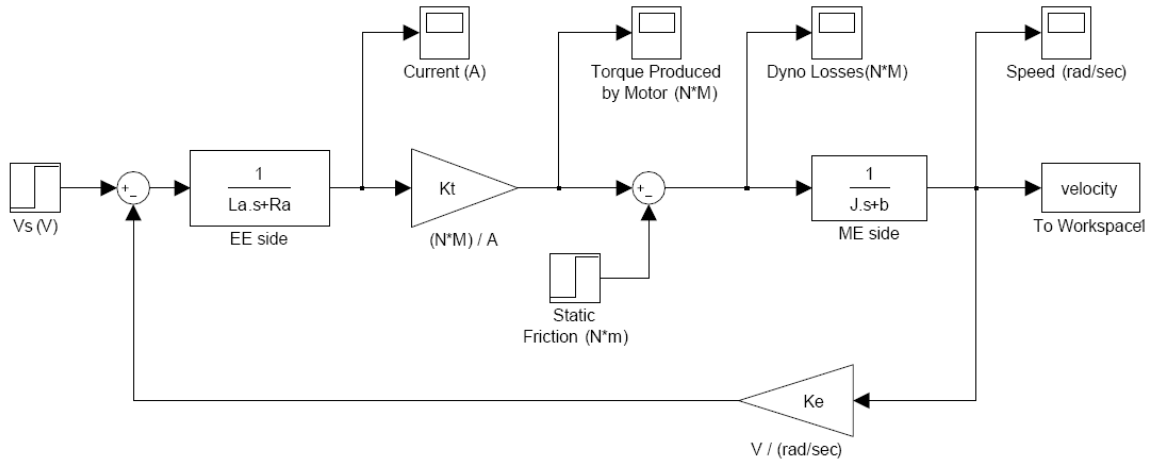


Figure 7 - Simulink PM DC Motor Model

a. Measurement of R_a and L_a

The locked rotor test was used to calculate the R_a and L_a . This test used the circuit shown in Figure 8 with an initial voltage of 0V and the knife switch in the closed position. Then, the voltage was slowly increased until the shaft of the motor started to rotate. With the motor rotating slowly, the voltage was decreased until the rotation stopped.

R_a is calculated by recording the source voltage (V_s) and the armature current (I_a) and using Ohm's law given in Equation 1.

$$R_a = \frac{V_s}{I_a}$$

Equation 1 - Armature Resistance Calculation

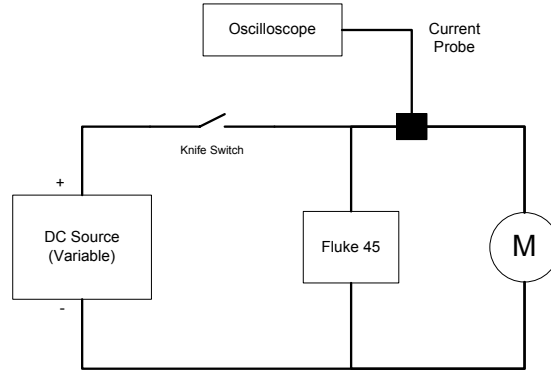


Figure 8 - Circuit to find R_a and L_a

The response of the armature current to a step input was used to calculate L_a . The oscilloscope was used to capture the response, shown in Figure 9, once the knife switch was closed. Finding the time constant from the plot, L_a was calculated using Equation 2.

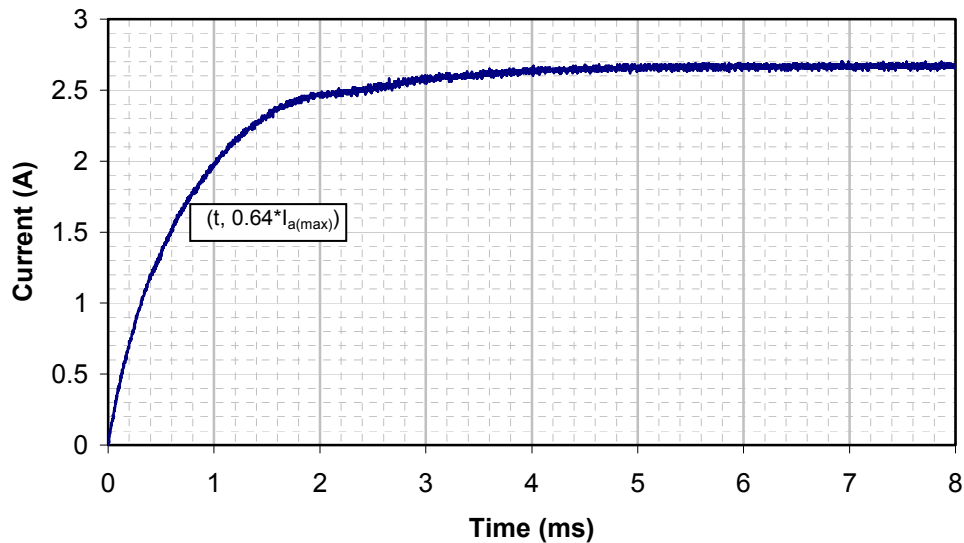


Figure 9 – Ramp Up Current for Locked Rotor Test

$$L_a = \tau_e R_a$$

Equation 2 - Equation to Calculate L_a

b. Measurement of Motor Constant, K_e and K_t

A mid-range no load speed test was performed, using the experimental setup shown in Figure 10, by setting the V_s equal to 12, which is $\frac{1}{2}$ the rated voltage of the motor. The

armature current, I_a , and motor speed, ω_s , were recorded and Equation 3 were used to find the constants. Equation 4 is only valid when using Standard International (SI) units.

$$Ke = Kt = \frac{Vs - IaRa}{\omega_s}$$

Equation 3 - Equation for Motor Constants

c. Measurement of $T_{S.F.}$ and b

A mid-range no load speed test was performed, again using the experimental setup shown in Figure 10, by setting the V_s equal to 1/3 and 2/3 rated voltage of the motor or 8V and 16V, respectively. The armature current, I_a , and motor speed, ω_s , were recorded and Equation 4 was used to find $T_{S.F.}$ and b by solving the 2 equations

$$T_{developed} - T_{S.F.} - b\omega_s = K_T I_a - T_{S.F.} - b\omega_s = 0$$

Equation 4 – Sum of All Torques

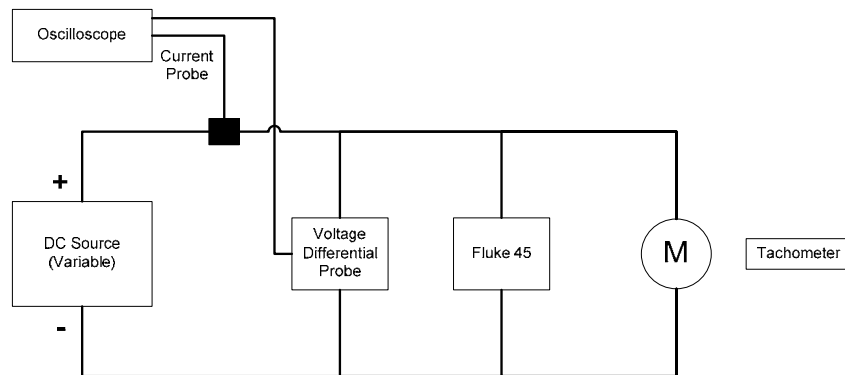


Figure 10 - Circuit Used for Motor Testing

d. Measurement of J

The coast down test was used to find J . To complete the coast down test, the motor was brought to full speed with the rated voltage of 24V and the oscilloscope was set to trigger on the falling edge with a trigger limit close to the rated voltage. The voltage source was then turned off and the emf voltage was captured by the oscilloscope. The data was saved and imported into excel. Equation 5 was used to find the time constant (τ) and Equation 6 was used to find J . The τ could be found at any point along the curve because it should have been linear. (Equation 5 is only valid for $\omega \geq 0$.)

$$\omega(t) = \frac{V_{emf}}{K_t} = \left[\frac{V_S}{K_t} + \frac{T_{SF}}{b} \right] e^{-t/\tau} - \frac{T_{SF}}{b}$$

Equation 5 – Summation of All Torques during Coast-Down

$$J = b\tau$$

Equation 6 – Mass Moment of Inertia

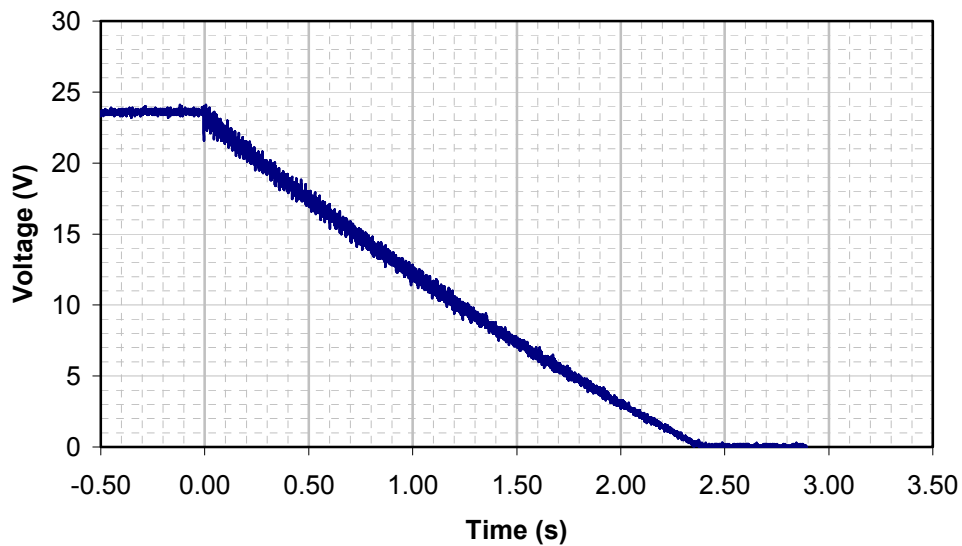


Figure 11 - Results of Coast-Down Test

e. Motor Characteristics Values

$$R_a = 0.045 \quad \Omega$$

$$L_a = 33.84 \quad \mu H$$

$$K_t = 0.063839 \quad \frac{N \cdot m}{A}$$

$$K_e = 0.063839 \quad \frac{V}{rad/sec}$$

$$T_{SF} = 0.129315 \quad N \cdot m$$

$$b = 0.000276 \quad \frac{N \cdot m}{rad/sec}$$

$$J = 0.001134 \quad Kg \cdot m^2$$

$$\tau = 4.11 \quad s$$

2. PM DC Motor Simulink Model

The motor model was created using Simulink and knowledge acquired in EE450 - Electronic Product Design. This model is for a Permanent Magnet DC Motor, which is shown in Figure 12.

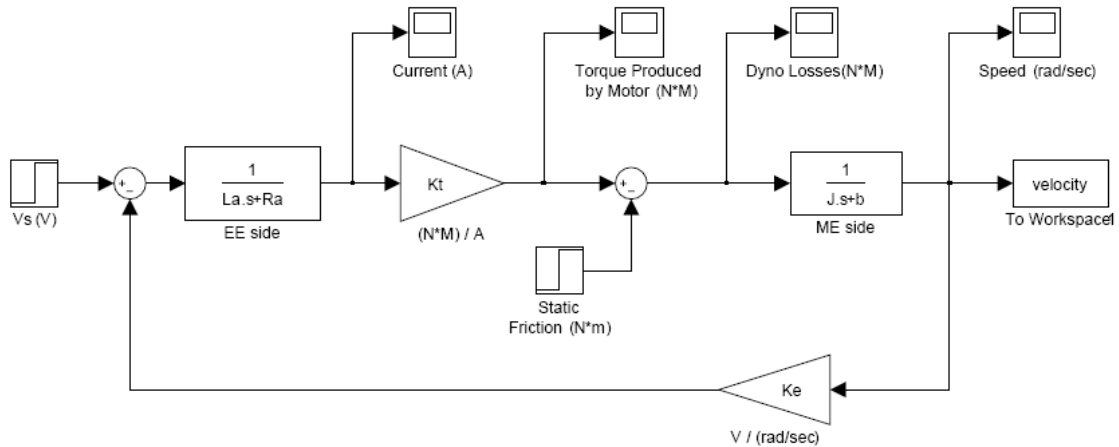


Figure 12 - Simulink Model for PM DC Motor

To confirm that the model was accurate, the team took experimental values with the circuit found in Figure 9 and compared the values with the Simulink values. These comparisons are shown in Table 2 and Figure 13. The comparison shows that the Simulink model is accurate to within 2.5%. This confirms that the model is good and the motor parameters are accurate.

Table 2 - Motor Simulation vs. Experimental Data

Fraction of Voltage	Experimental				Simulink		Simulink vs. Experimental error
	Voltage (V)	Current (A)	RPM	ω (rad/sec)	Current (A)	ω (rad/sec)	
1	24	3.60	3535	370.2	3.64	374.8	-1.25%
3/4	18	3.18	2660	278.6	3.23	281.0	-0.88%
2/3	16	3.10	2373	248.5	3.10	249.9	-0.56%
1/2	12	2.80	1776	186.0	2.83	187.4	-0.76%
1/3	8	2.56	1180	123.6	2.56	124.9	-1.08%
1/4	6	2.45	883	92.5	2.42	93.7	-1.33%
1/6	4	2.35	583	61.1	2.29	62.4	-2.21%

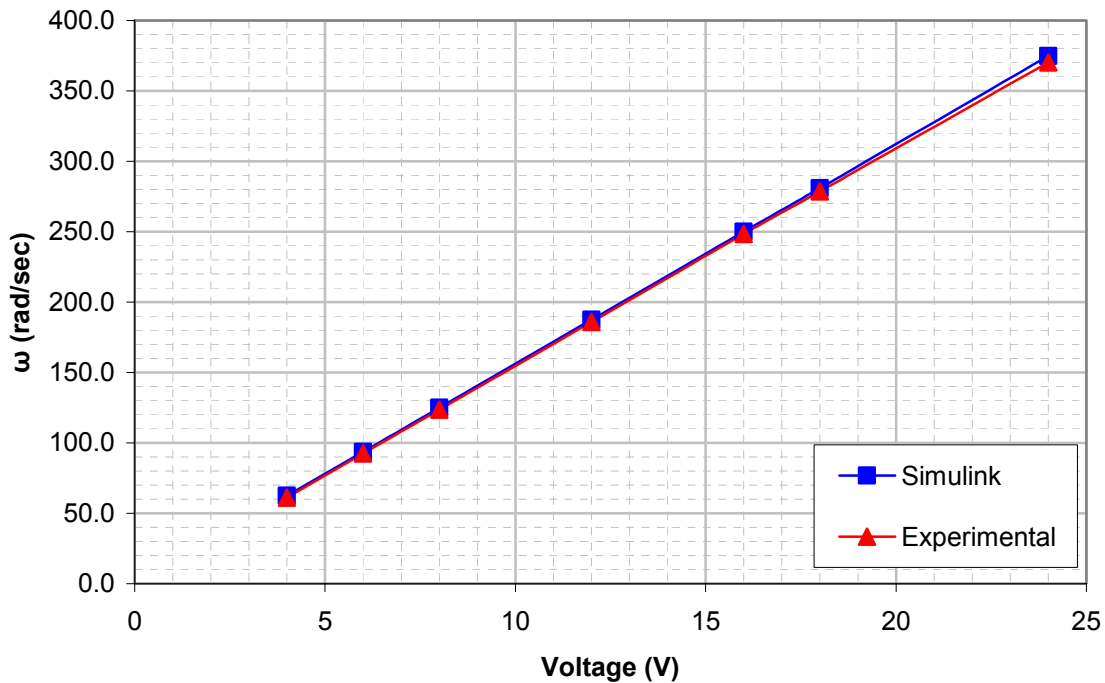


Figure 13 - Graph of Simulink vs. Experimental for Motor Only

B. Mower System

The mower system was implemented by integrating the motor, batteries, blade, and controls on a mower deck. An important goal was safety and ease of measurement during testing. The controls were a pull handle as a safety switch and a main disconnect switch.

1. Safety Considerations

When implementing the mower system, safety had to be taken into consideration and, consequently, the team added a manual on/off safety switch and a pull bar safety switch.

a. Manual On/Off Safety Switch

As part of the safety specifications, an on/off switch was added to the system to disconnect the batteries while the system was not in use. The switch could also be used to shut the system down in the case the pull bar safety switch failed to open the circuit. Also, the switch was wired into the system to break the series connection of the batteries on the mower and allow parallel charging by the Prostar charger. This was necessary since the PV array only generated 17.5V.

b. Pull Bar Safety Switch

In addition to the manual disconnect switch, a pull bar safety switch, which controlled a circuit breaker, was used for motor starting and stopping. The circuit breaker, shown in Figure 15, was also used as protection for the motor. Figure 14 shows the types of delays which the team could select from while making the decision on which delay and breaker rating to use. Ideally the type 56 delay should be used with the 35 amp rated breaker. By using the 35 Amp rated breaker, the system will have sufficient protection. Due to the delivery time on the type 56 breaker, the team could not obtain the breaker in time and the 40 Amp breaker described below was used instead. Though not ideal it was adequate for testing purposes.

The 40 Amp breaker used did not have a low enough rating for our application because $40 \text{ Amps} * 125\% = 50 \text{ Amps}$. By using the information in Figure 14, the 40 amp breaker with the type 34 delay might not even trip for about six minutes. Since the motor is only rated to run at 41 Amps continuously, this Carlington circuit breaker will not sufficiently protect the motor. The higher rated circuit breaker with the type 34 delay was only useful for testing purposes and should not be used in the final system.

A, B, C & D-SERIES TIME DELAY VALUES											
TRIP TIME (SECONDS)	PERCENT OF RATED CURRENT										
	DELAY	100%	125%	135%	150%	200%	400%	600%	800%	1000%	1200%
10	No Trip	May Trip	—	.032 MAX	.024 MAX	.020 MAX	.018 MAX	.016 MAX	.015 MAX	.013 MAX	.013 MAX
11	No Trip	.013 - .125	—	.010 - .070	.008 - .032	.006 - .020	.005 - .020	.004 - .020	.004 - .020	.004 - .020	.004 - .020
12	No Trip	.500 - 6.50	—	.300 - 3.00	.130 - 1.20	.031 - .220	.011 - .120	.004 - .090	.004 - .060	.004 - .040	.004 - .040
14	No Trip	2.00 - 60.0	—	1.20 - 40.0	.600 - 20.0	.150 - 3.00	.030 - 1.30	.004 - .600	.004 - .100	.004 - .100	.004 - .100
16	No Trip	45.0 - 345	—	20.0 - 150	9.00 - 60.0	1.40 - 11.4	.150 - 5.80	.009 - 3.70	.005 - 1.70	.005 - 1.500	.005 - 1.500
20	No Trip	May Trip	—	.040 MAX	.035 MAX	.030 MAX	.025 MAX	.020 MAX	.017 MAX	.015 MAX	.015 MAX
21	No Trip	.014 - .150	—	.011 - .095	.008 - .055	.006 - .035	.005 - .027	.005 - .021	.004 - .018	.004 - .017	.004 - .017
22	No Trip	.700 - 12.0	—	.350 - 4.00	.130 - 1.30	.027 - .220	.008 - .130	.004 - .090	.004 - .045	.004 - .040	.004 - .040
24	No Trip	10.0 - 160	—	6.00 - 60.0	2.20 - 20.0	.300 - 3.00	.050 - 1.30	.007 - .500	.005 - .060	.005 - .040	.005 - .040
26	No Trip	50.0 - 700	—	32.0 - 350	10.0 - 90.0	1.50 - 15.0	.500 - 7.00	.020 - 3.00	.006 - 2.00	.005 - 1.00	.005 - 1.00
32	No Trip	May Trip	.400 - 8.00	.300 - 4.00	.130 - 1.30	.027 - .220	.008 - .130	.004 - .090	.004 - .060	.004 - .040	.004 - .040
34	No Trip	May Trip	1.80 - 100	1.20 - 60.0	.600 - 20.0	.150 - 3.00	.030 - 1.30	.004 - .600	.004 - .110	.004 - .100	.004 - .100
36	No Trip	May Trip	35.0 - 520	20.0 - 350	9.00 - 90.0	1.40 - 15.0	.150 - 7.00	.009 - 3.70	.005 - 2.00	.004 - 1.00	.004 - 1.00
42	No Trip	.700 - 12.0	—	.400 - 6.00	.180 - 2.30	.050 - .600	.026 - .300	.018 - .200	.014 - .150	.012 - .130	.012 - .130
44	No Trip	7.00 - 100	—	3.00 - 50.0	1.10 - 18.0	.220 - 3.00	.120 - 1.70	.075 - 1.20	.050 - .850	.042 - .720	.042 - .720
46	No Trip	50.0 - 700	—	31.0 - 350	12.0 - 150	1.50 - 20.0	.700 - 10.0	.404 - 7.90	.260 - 6.50	.198 - 5.80	.198 - 5.80
52	No Trip	.500 - 6.50	—	.340 - 4.50	.180 - 2.30	.051 - .600	.030 - .320	.018 - .220	.014 - .200	.012 - .130	.012 - .130
54	No Trip	1.50 - 50.0	—	.750 - 35.0	.350 - 18.0	.110 - 3.00	.070 - 1.70	.045 - 1.40	.039 - 1.30	.035 - 1.30	.035 - 1.30
56	No Trip	45.0 - 345	—	19.0 - 170	8.50 - 100	1.24 - 15.0	.410 - 9.00	.256 - 8.00	.210 - 5.50	.198 - 2.90	.198 - 2.90

Figure 14 – Time Delay Values for Carlington Breakers

Another major part of implementing the Pull Bar safety switch was the actual fabrication of the platform in which it was housed. Figure 15 shows how the breaker was mounted in order for the Pull Bar safety switch to be utilized. The team found this idea for mounting at Mr. Lee's website:

<http://www.builditsolar.com/Projects/Vehicles/LeeMower.htm>

The team made a few adjustments, but the pull bar switch is basically the same idea that Mr. Lee used on his lawn mower conversion project.

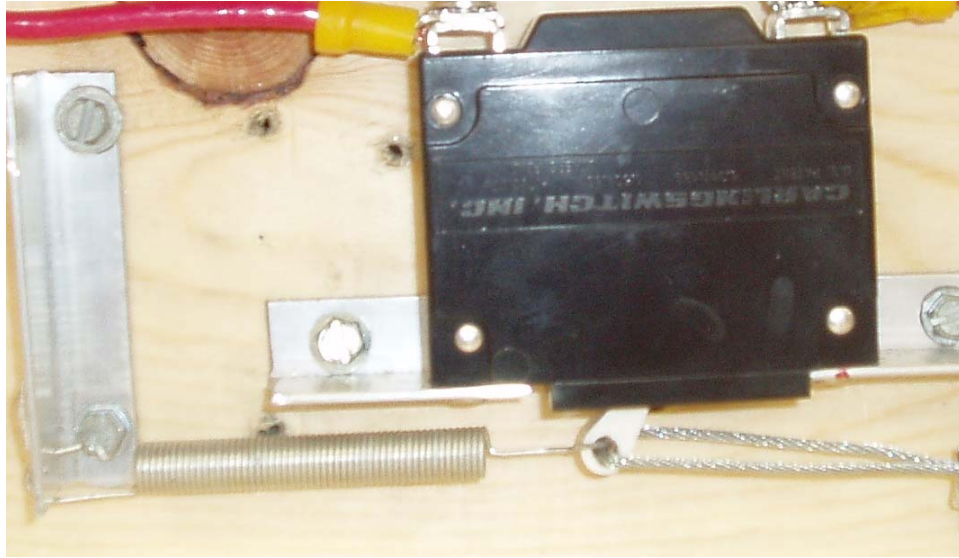


Figure 15 – Pull Bar Safety Switch for Motor Starting

As shown in Figure 15, a spring is connected to the breaker handle to hold the breaker in the off position until the safety switch is activated by the user. Once the user releases the Pull Bar, the spring supplies enough tension to return the breaker to the off position. If this item fails, the manual disconnect switch can be used to shut the system down. It was determined that a throttle cable could not be used because it was too rigid, which could cause a twisting force on the handle of the circuit breaker. Therefore the throttle cable was replaced with a 1/6 inch stranded steel cable that was threaded into the sheathing of the throttle cable.

2. Mower System Simulation

The goal of the mower simulation is to calculate the power required to cut different height and density grass. In order to find the cutting power, an accurate model of the mower system was created. The mower system simulation incorporated the Simulink motor model found in the prior section, IR losses of the batteries, mass moment of inertia of the blade, and force (N*m) needed to spin the blade on cement.

The motor model, found in Figure 7, was used at the starting point of the mower system model. Since the batteries have IR losses, these losses were subtracted from the voltage applied to the EE side of the motor model. The cutting blade was modeled using two different variables; mass moment of inertia of the blade (J_b) and force needed to spin the blade (T_{spin}). T_{spin} included the friction caused by wind resistance caused by spinning the blade. The cutting force ($T_{cutting}$), along with the T_{spin} , was subtracted from the system between the torque constant and the ME side blocks shown in Figure 16 and 17.

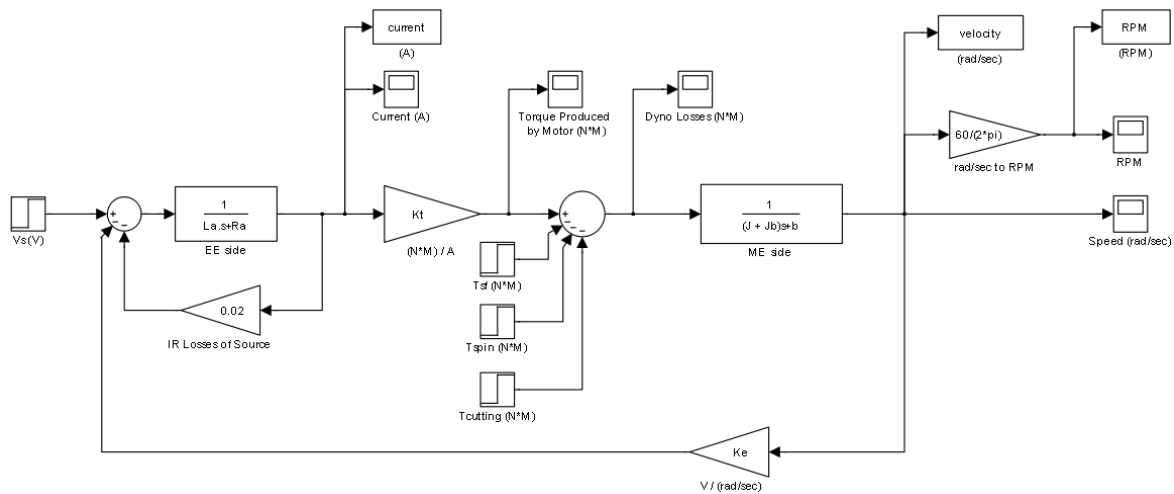


Figure 16 - Mower System Simulation

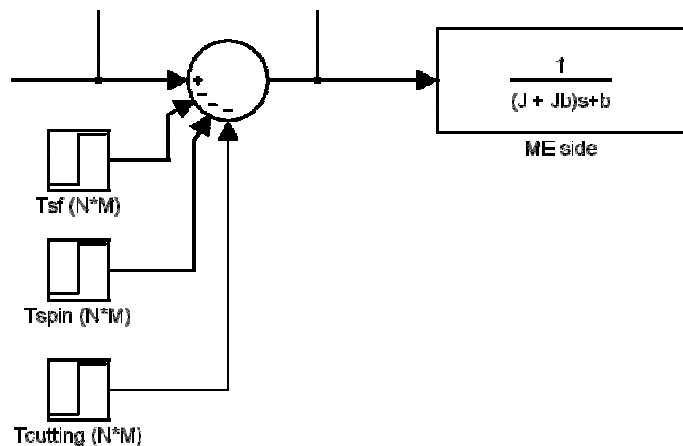


Figure 17 - Force Terms for Simulation

a. Measurement of J_b

The mass moment of inertia of the blade and the blade assembly was found by using mass moment of inertia Equations found at <http://www.livephysics.com/Tables-of-physical-data/mechanical/moment-of-inertia.html>. Since the blade assembly was a solid cylinder, the solid cylinder mass moment of inertia with a central axis, Equation 7, was used to compute the mass moment of inertia value for the blade assembly. The next step was to find the mass moment of inertia of the blade. The mass moment of inertia of the blade was found by using the rectangular plate with the axis through the center Equation, Equation 8, from the live physics website. Once the mass moment of inertia was found

for both the blade and the blade assembly, these terms were combined to form the J_b term.

$$J = \frac{1}{2}MR^2$$

Equation 7 – Mass Moment of Inertia for Solid Cylinder with Central Axis of Cylinder

$$J = \frac{1}{12}M(a^2 + b^2)$$

Equation 8 – Mass Moment of Inertia for Rectangular Plate with Axis through Center

b. Measurement of T_{spin}

Since T_{spin} is the value needed to spin the blade only and not cutting grass; the team took readings for the mower system when the blade was spinning over cement. The experimental voltage value was entered into the mower system model, making sure that J_b was included and $T_{cutting}$ was set to 0. The T_{spin} value was increased until the model current was the about the same as the experimental value. This was done on multiple samples (yellow highlighted values in Table 5 for the 19 inch blade and Table 6 for the 22 inch blade) and those samples were averaged to find the T_{spin} value that was used in the mower system model. The T_{spin} average values found were 0.728 N*M for the 19 inch blade and 1.433 for the 22 inch blade.

b. Measurement of $T_{cutting}$

The cutting force was found in a similar fashion as T_{spin} . The team first entered the J_b and T_{spin} values into the mower system model in Figure 16 and then increased the $T_{cutting}$ value until the current was the same as the experimental value. This process was completed for all of the individual experimental samples, results shown in Table 5 and 6.

3. Field Test Data Collection

After the mower system was implemented with all of the necessary safety features in place, data was collected for two different sized metal blades. A field test was performed with a 19” and 22” blade, the test data can be found in Tables 3 and 4, respectively.

Table 3 - 19 inch Field Test Data

Field Test		Outside Conditions: Partly Cloudy, 79°F, Wind SSW 26 MPH 4/26/2009 15:00		
Sample	Mowing Conditions	Current (A)	Voltage (V)	Watts (W)
1	Medium grass density, motor warm, standing still	14.75	21.98	324.2
2	On cement, motor cold, standing still	15.06	24.23	364.9
3	Cutting 3 inches of grass, medium grass density, walking	19.10	23.60	450.8
4	Cutting 4 inches of grass, medium grass density, walking	25.64	21.26	545.1
5	Cutting 3 inches of grass, medium grass density, walking fast	31.55	23.64	745.8
6	Cutting 4 inches of grass, high grass density, walking	34.25	22.93	785.4
7	Cutting 5 inches of grass, high grass density, walking	36.21	22.93	830.3
8	Hit tree root, walking	43.55	21.35	929.8
Average running current		25.2	22.9	578.1

Table 4 - 22 inch Field Test Data

Field Test		Outside Conditions: Partly Cloudy, 59°F, Wind SSW 16 MPH 4/16/2009 15:00		
Sample	Mowing Conditions	Current (A)	Voltage (V)	Watts (W)
1	On cement, motor cold, standing still	25.64	23.82	610.7
2	On cement, motor warm, standing still	26.32	23.53	619.3
3	Cutting 3 inches of grass, medium grass density, standing still	27.60	23.66	653.0
4	Cutting 3 inches of grass, high grass density, peak#1	36.15	23.24	840.1
5	Cutting 3 inches of grass, high grass density, peak#2	38.60	23.25	897.5
6	Cutting 3 inches of grass, medium grass density, walking	31.00	23.25	720.8
7	Cutting 3 inches of grass, thick patch of grass, walking	40.00	22.10	884.0
8	Cutting 3 inches of grass, high grass density, peak#3	45.00	22.00	990.0
9	Cutting 3 inches of grass, thick grass density, walking	34.53	21.86	754.8
10	Cutting 5 inches of grass, medium grass density, standing still	28.41	22.49	638.9
11	Cutting 5 inches of grass, high grass density, peak#4	48.00	22.46	1078.1
12	Cutting 5 inches of grass, medium grass density, walking	30.00	22.45	673.5
Average running current		35.5	22.8	806.9

As seen in Table 3 and in Table 4, the 22" blade cuts a 34% larger area at a 60% increase in power. The data shows the average value of current measured for the 19 inch blade was about 19 Amps and the average value measured for the 22 inch blade was about 31 Amps. Over all, the 19 inch blade used about 1/3 less current than the 22 inch blade and roughly one half of the force to spin the three inch shorter blade as seen in Table 5 and 6.

4. Cutting Power Calculation

Experimental values were taken in the field and recorded. The values were then used to compute T_{spin} , $T_{cutting}$, and Estimated Spinning Power. T_{spin} and $T_{cutting}$ values were found by utilizing the Simulink model shown in Figure 16. The estimated spinning power was acquired by averaging the power in samples 1 and 2 of Table 3 for the 19 inch blade. The same process was repeated for the 22 inch blade with the information given in Table 4. The results are 344.55 W for 19 inch blade and 615.00 W for the 22 inch blade. The estimated cutting power was then found by subtracting the average spinning power values found from the power for every other sample in Table 3 and 4. The values found were updated, and the new information was added to Tables 5 and 6 for the 19 inch blade and 22 inch blade, respectively. The preferred configuration is the one that will have the best $T_{cutting}$ to T_{spin} ratio.

Table 5 - 19 inch Blade Force Approximations

Field Test					Outside Conditions: Partly Cloudy, 79°F, Wind SSW 26 MPH 4/26/2009 15:00		
Sample	Mowing Conditions	Current (A)	Voltage (V)	Watts (W)	Calculated		Cutting Power
					Tspin (N*M)	Tcutting (N*M)	Estimated Watts (W)
1	Medium grass density, motor warm, standing still	14.75	21.98	324.2	0.725	N/A	N/A
2	On cement, motor cold, standing still	15.06	24.23	364.9	0.730	N/A	N/A
3	Cutting 3 inches of grass, medium grass density, walking	19.10	23.60	450.8	0.728	0.260	106.2
4	Cutting 4 inches of grass, medium grass density, walking	25.64	21.26	545.1	0.728	0.685	200.6
5	Cutting 3 inches of grass, medium grass density, walking fast	31.55	23.64	745.8	0.728	1.050	401.3
6	Cutting 4 inches of grass, high grass density, walking	34.25	22.93	785.4	0.728	1.240	440.8
7	Cutting 5 inches of grass, high grass density, walking	36.21	22.93	830.3	0.728	1.380	485.7
8	Hit tree root, walking	43.55	21.35	929.8	0.728	1.650	585.2
Average running current		25.2	22.9	578.1			326.9

Not Included for Averages

Standing still on cement

Table 6 - 22 inch blade Force Approximations

Field Test					Outside Conditions: Partly Cloudy, 79°F, Wind SSW 26 MPH 4/26/2009 15:00		Calculated	Cutting Power
Sample	Mowing Conditions	Current (A)	Voltage (V)	Watts (W)	Tspin	Tcutting	Estimated	
					(N*M)	(N*M)	Watts (W)	
1	On cement, motor cold, standing still	25.64	23.82	610.7	1.410	N/A	N/A	
2	On cement, motor warm, standing still	26.32	23.53	619.3	1.455	N/A	N/A	
3	Cutting 3 inches of grass, medium grass density, standing still	27.60	23.66	653.0	1.433	0.108	25.3	
4	Cutting 3 inches of grass, high grass density, peak#1	36.15	23.24	840.1	1.433	0.656	212.5	
5	Cutting 3 inches of grass, high grass density, peak#2	38.60	23.25	897.5	1.433	0.814	269.8	
6	Cutting 3 inches of grass, medium grass density, walking	31.00	23.25	720.8	1.433	0.326	93.1	
7	Cutting 3 inches of grass, thick patch of grass, walking	40.00	22.10	884.0	1.433	0.903	256.3	
8	Cutting 3 inches of grass, high grass density, peak#3	45.00	22.00	990.0	1.433	1.234	362.3	
9	Cutting 3 inches of grass, thick grass density, walking	34.53	21.86	754.8	1.433	0.556	127.2	
10	Cutting 5 inches of grass, medium grass density, standing still	28.41	22.49	638.9	1.433	0.164	11.3	
11	Cutting 5 inches of grass, high grass density, peak#4	48.00	22.46	1078.1	1.433	1.421	450.4	
12	Cutting 5 inches of grass, medium grass density, walking	30.00	22.45	673.5	1.433	0.266	45.8	
Average running current		35.5	22.8	806.9			227.2	

Not Included for Averages Standing still on cement

C. Battery

The major factors in battery selection are weight, price, and capacity. The battery capacity is determined based on the information in Table 1. Sample number 2 data are used again to size the battery appropriately. The capacity of the battery was selected based on the restriction that the battery will only be 80% discharged after an hour of operation delivering the sample 2 power of 453 watts. Thus, the battery capacity is computed using Equation 9 which yields 23.58 amp-hours.

$$(\text{System Voltage}) * (0.80 * \text{Battery Capacity}) = (\text{Calculated Power needed}) * (1 \text{ hour})$$

Equation 9 – Required Battery Capacity

The SVR brand of batteries, found at <http://www.nprobotics.com>, offers deep discharge AGM lead acid batteries in several capacities. The 22 amp-hour battery weighs 18.8lbs and the 28 amp-hour battery weighs 23.5 lbs. In consideration of the goal to design for low weight, the team chose the 22 amp-hour battery (NPC-B1812) for the mower application. The system uses two NPC-B1812 batteries in series to obtain the 24 volts needed for the selected motor yielding an overall weight of 37.6 lbs.

D. PV Charging

The first cut photovoltaic sizing and charging time calculation is based on battery capacity and isolation data. From the calculations done in section B, it was found that an 80% discharged battery is depleted of 453 WH (watt-hour) or about 1630 kilojoules of energy. System functional requirements dictate that the PV array charge the batteries and restore the lost energy in 3 days or less in June. The Equations showing the relation between PV array parameters (area and efficiency), solar radiation levels (denoted PVradiation), and time to charge are given in Equations 10 and 11. The PV radiation is dependent on tilt and orientation of the panel. For the calculation presented in this section, tilt and orientation was chosen as a south facing plate at an angle of latitude + 15°. For this tilt and orientation, values for minimum average energy density per day (in kWh/m²/day) for regions of the U.S. were found from http://rredc.nrel.gov/solar/old_data/nsrdb/redbook/atlas/Table.html. In the case of PV array parameters, the panel purchased for the prior project (BP 350) was used as a guide. This panel has an efficiency of 10% and an area of 0.45 m². Using these values, the days needed to supply 1630 kilojoules of energy was computed for three different values of energy density per day. The value of 4 kWh/m²/day is valid for most of the U.S. and the lower value is valid for New England and small regions of northern Minnesota, Wisconsin, and Michigan. The calculation for of 4 kWh/m²/day radiation value is shown as Equation 12.

The results of the computation are shown in Table 7 and indicate the BP 350 PV array will meet the charging time specification in most of the U.S. in June. Also, the charging system must also charge the batteries within 7 days in the months of September and May. Figures 26 and 27, given in the Appendix, show the minimum radiation for these months again ranges from 3 kWh/m²/day to 5 kWh/m²/day but with more of the U.S. receiving the small value of radiation. Thus Table 7 shows that the worst case time needed to charge during May and September is 3.4 days, which is significantly less than the 7 day requirement. It is important to note that the preceding calculations assume the charging controller has no losses and 100% of the energy from the PV array is transferred to the batteries.

$$PVarea(m^2) * PVradiation \left(\frac{kWh}{m^2 \cdot day} \right) * eff * 1000 \left(\frac{W}{kW} \right) * 1 \left(\frac{J/s}{W} \right) * 3600 \left(\frac{s}{hr} \right) = \frac{J}{day}$$

Equation 10 – PV output (J/day)

$$\frac{BatteryEnergy(J)}{DailyEnergyAvailable \left(\frac{J}{Day} \right)} = DaysNeededToCharge$$

Equation 11 – PV System, days needed to charge battery

$$0.450543(m^2) * 4 \left(\frac{kWh/m^2}{day} \right) * 10\% * 1000 \left(\frac{W}{kW} \right) * 1 \left(\frac{J/s}{W} \right) * 3600 \left(\frac{s}{hr} \right) = 648781.92 \left(\frac{J}{day} \right)$$

$$\frac{1630800(J)}{648781.92 \left(\frac{J}{Day} \right)} = 2.5(DaysNeededToCharge)$$

Equation 12 – Days needed to charge battery for 4kWh/m2/day radiation

Table 7-Photovoltaic Sizing Information with radiation data collected from <http://sel.me.wisc.edu/trnsys/weather/weather.htm>

Photovoltaic Sizing Information			
Month	Minimum Radiation (kWh/m2/day)	PV Output (Joules/day)	Time Needed to Charge (days)
June	3	486586.44	3.4
	4	648781.92	2.5
	5	810977.40	2

E. Charging System Implementation

The charging system was tested in phases by the team. The relays were tested first. Next the current sensor voltage output was tested. After the relays and current sensors were tested the EMAC controller was tested with an analog input imitating the current sensor outputs. Once the EMAC controller worked with an analog input, the overall system was ready for a final test.

1. Charging System Wiring Diagram

The charging system consisted of the blocks, identified in Figure 18, implemented with mostly off-the-shelf components. The function and requirements of these components are as follows.

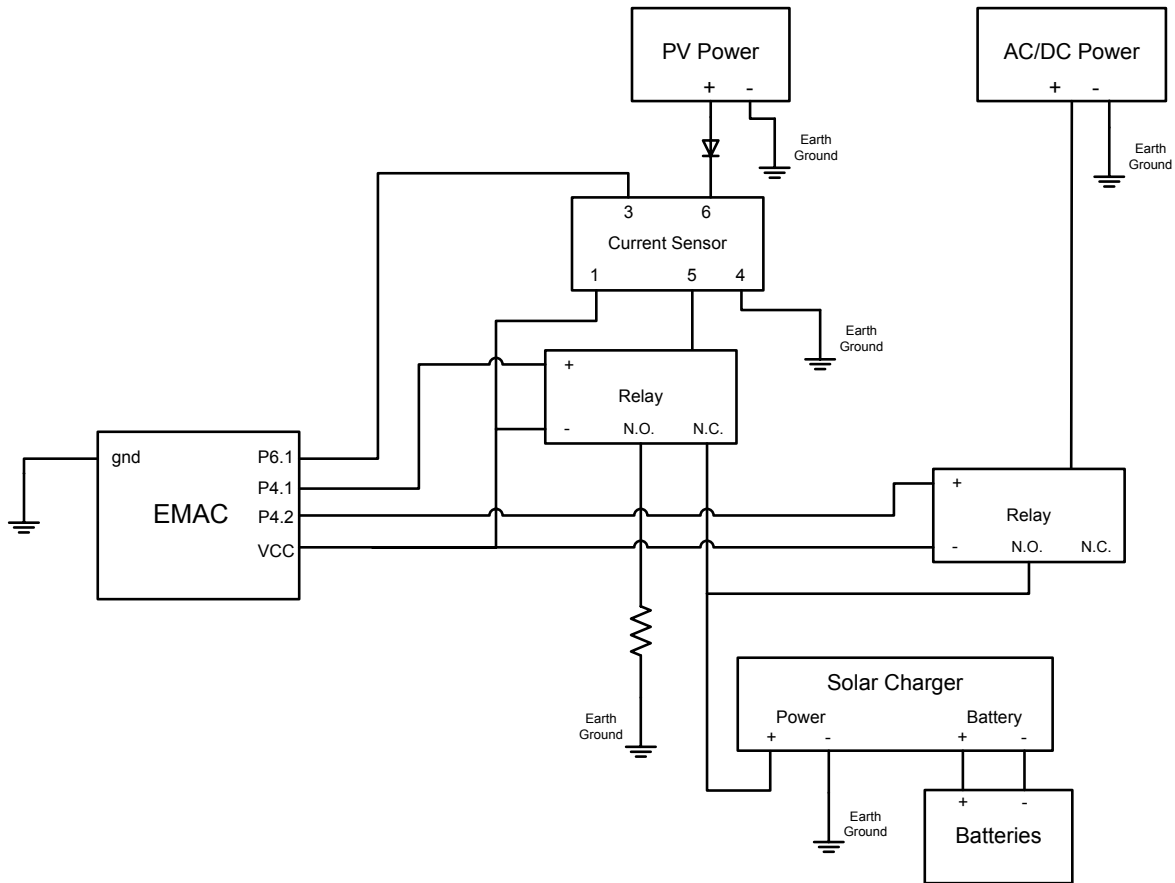


Figure 18 – Charging System Wiring Diagram

Charging System Components

PV: LCFELM 2008 used the BP 350 solar panel. This panel was used by the 2007 team and, as discussed in Subsection E, meets the minimum charging functional requirements.

AC/DC Power supply: The team specified that the system would charge in 4 days. Since there are some days that provide limited solar radiation, DC backup power was needed. The Sunforce AC to DC Power converter, with a max output of 5.8 amps at 12 volts, was used to supply this function.

Diode: For PV protection the team decided to use the 1N344A diode. This ensures the AC power will not back feed the PV. The diode is rated for 10amps.

Current sensor: Sensing the current available from the PV was essential to the charging system. The group wanted a system that was low carbon footprint while also being smart.

To sense current the team needed a current sensor that could output an analog voltage between 0 and 5 volts with a 0 to 3 amp input. The SCD03PUR made by CUI Inc. outputs 0 to 5 volts with a -3 to 3 amp input and can withstand 30 amps for 50ms.

Relays: In order for the system to switch between PV power and AC power the charging system needed relays that could withstand 3 amps and have both a normally closed and normally open contact. The G6RL15VDC SPDT made by Omron withstands 5 amps at 24VDC, and has both a N.C. and N.O. contact.

Solar Charger controller: The team found the Pro-Start 15 solar charging controller. The charger can change the charging scheme based on the three common lead acid batteries available. The charger withstands a 15 amp maximum with a PV input. The charger specifies that inputs should be PV only so our AC/DC power supply had to be similar to the specifications of the PV.

EMAC: The EMAC measures the voltage output of the current sensor, which is proportional to the current through the sensor, to determine if the system needs to use solar power or DC backup power. For the first three days the EMAC does not control the relays. During this time the PV array is the only available source of power. Once three days has passed the system checks the current available from the PV array. If the current drops below .5amps the system switches to AC Power. After AC Power has been activated the system checks the current from the PV array through the dummy load. Once the current raises above 1amp the system switches back to PV power. This cycle continues until the user stops the system.

Batteries: As discussed in Section C, the NPC-B1812 12V, 22Ah batteries were selected. The PV array and the charging algorithm were designed to charge these batteries in no more than 4 days.

2. Current Sensor Testing

In order to setup the charging system threshold values, the analog output from the current sensor was measured using both the circuit, shown in Figure 19, for low current values as well as the PV for high current values. The results are given in Table 8 and Figure 20.

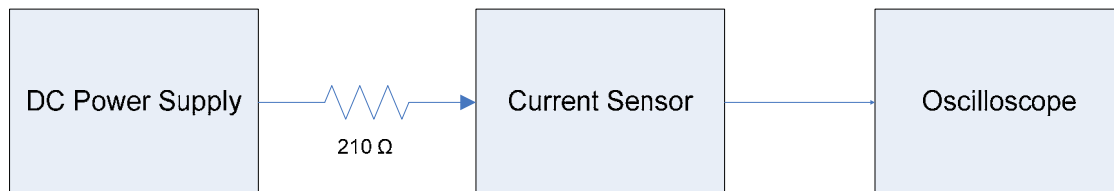


Figure 19 - Current Sensor Testing Diagram

Table 8 - Current Sensor Data

Current	Voltage
0.2	2.6
0.4	2.7
1.0	3.2
1.5	3.5
2.0	3.8
3.1	4.8

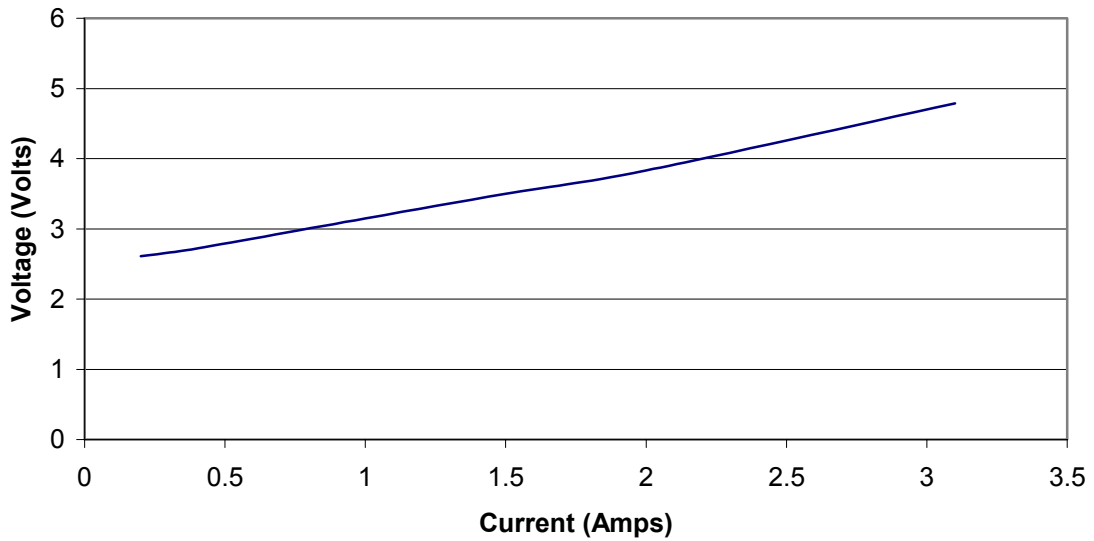


Figure 20 – Graph for Current Sensor Output

The team wanted a low current threshold of .5 amps and a high current threshold of 1 amp. Using Figure 20, these currents translate in to voltages of 2.6 and 3.1, respectively.

3. Relay Testing

The relays were tested by using the EMAC board. A simple code that switched the relays on and off through pins 4.1 and 4.2 was used. A simplified test set up is shown in Figure 21.

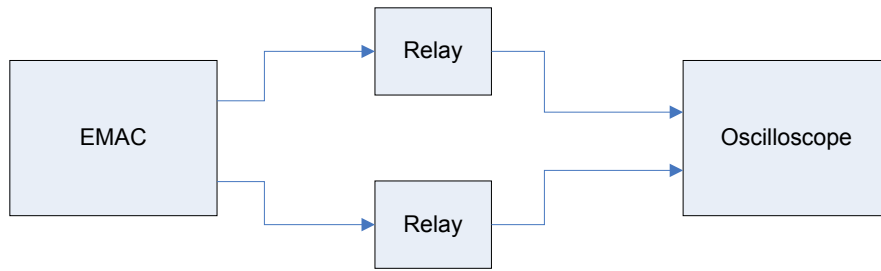


Figure 21 - Relay Testing Diagram

4. Combined Component Testing Without Current Sensor

During the first initial tests of the charging system the team used a DC power supply for the simulated current sensor inputs as shown in Figure 22. This allowed the input voltage to be easily controlled. When the DC voltage was decreased below the low threshold, the system switched the relays to the AC setting. Also, when the DC voltage was increased above the high threshold, the system switched the relays to the PV setting.

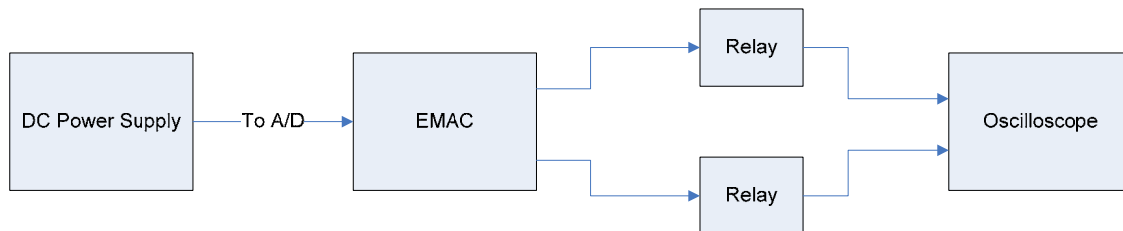


Figure 22 - System Testing Diagram

5. Complete Charging System Testing

Once the system was working with the AC supply, the team connected the complete charging system. Figure 4 shows the entire system block diagram. The charging system will only operate from the PV for the first 72 hours and then switch between PV and AC back up thereafter. Due to this constraint, hard coding was necessary for testing purposes. After the system was connected, the system operation was verified. Ammeters connected in series with the PV power and AC power inputs were monitored to check the current status of the system. While the system was on PV there was current through the PV relay, but not the AC relay. When the system was switched to AC power there was no current through the PV relay and there was current through the AC relay.

IV. Results

The results of the project were compiled and entered into this section. The project was broken into Mower and Charger systems.

Mower System Results

The mower system was implemented as shown in Figure 2. A testing platform was successfully constructed and used to perform field tests using a 22 inch blade as well as a 19 inch blade. The 22 inch blade cut well but was not able to fulfill the system requirement of running for 1 hour. The mower only ran for 40 minutes with the 22 inch blade. As a solution to the problem, the team used a 19 inch blade. The 19 inch blade satisfied both the one hour running time requirement and the 10,000 square feet requirement. A successful Simulink model was implemented and utilized to calculate the amount of power needed to cut the grass. The results using this model to analyze the field data are in Table 5 and Table 6. The power used to cut the grass was also estimated in Table 5 and Table 6. Overall, the mower system was a huge success. After replacing the 22 inch blade with the 19 inch blade, the mower met most the requirements. The Batteries still are too heavy due to the current technology being used. A high energy-density to weight ratio battery will have to be used.

Charger System Results

The solar charger system was implemented as shown in Figure 4. During the first three days the charger stayed on PV Power. Once three days passed the system switched the relays to AC Power when the current from the PV array fell below .5amps. After the current from the PV array reached 1amp the system switched the relays back to PV Power. If the user pressed "A" the system went to the stop module. In the stop module the user had to press "1" to go back to PV Power, "2" to go back to AC Power, or "C" to reset the system. The system was fully operational by the end of the project. Power from the PV array and DC Power supply was fed into the charger controller to verify the operation of the system. On a sunny day the PV Power was on with a clock that had passed 72hours. When the PV array was covered with a piece of paper to simulate a cloud, the system switched to AC Power. After the piece of paper was removed the system switched back to PV Power. The only problem with the current charging system is that once three days has passed AC Power can be on, but the batteries might already be charged. The system needs to have a way of sensing when the batteries are fully charged.

V. Recommendations for Future Work

The project was able to integrate the mower system and the charging systems to get a functional product. The following are the opportunities for future work on the mower system and the charging system.

Mower System Recommendations

- Decrease the mower deck size to reduce power consumption. The 19 inch blade had a significant less amount of power consumption compared to the 22 inch blade.
- Operating the blade at a slower controlled speed will allow the efficiency to increase. The target efficiency range on the DC motor used is 2800 RPM (found at http://www.cloudelectric.com/product_p/mo-4bb3995.htm) and a controller could be added to control the system at the desired operating speed.
- Using different battery technology would greatly reduce the weight of the system. If NiMH Rechargeable M-Size Cells were used, the weight of the system would be greatly reduced. More information can be found about the M-Size Cells at: <http://www.batteryspace.com/index.asp?PageAction=VIEWPROD&ProdID=4934>.

Charger System Recommendations

- Design circuitry or implement electronics to sense the status of the battery during charging. This is important in order to make the charging system more efficient.
- Design a battery charger for NiMH batteries which can operate with the current system. This would be a great addition if the NiMH batteries are used to reduce the weight of the system

VI. Parts List

An estimated parts list was compiled so the team would be able to purchase the major components and to give time for delivery. This parts list will change as the project moves forward.

Table 9 - Pricing for Parts Used

Part Name	Quantity	Unit Price	Total Price
Motor Scott Upgrade 1+ HP "Electrathon"	1	\$349.00	\$349.00
12V 22Ah Lead Acid Battery	2	\$99.00	\$198.00
BP 350 - 50 Watt Photovoltaic Module	1	\$269.00	\$269.00
PS-15: Solar Charger for Lead Acid Battery	1	\$99.00	\$99.00
Mower Frame - Estimated Price	1	\$20.00	\$20.00
AC/DC Converter	1	\$9.00	\$9.00
Microcontroller - ATMEGA 168	1	\$2.39	\$2.39
LCD Display - MDLS-24269-HT-HV-S	1	\$5.00	\$5.00
Microcontroller Keypad	1	\$15.00	\$15.00
Safety Switch – 8125SHZBE	1	\$2.56	\$2.56
Relay – G6RL1	2	\$1.38	\$2.76
Current Sensors – SED03PUR	1	\$26.03	\$26.03
Carlinton Circuit Breaker – 40A, 34 delay	1	\$24.51	\$24.51
Doc Wattson Meter	1	\$59.95	\$59.95
		Total	\$1,079.44

The pricing for the lawn mower was found using single unit pricing, shown in Table 9.

VII. Patents

A patent is a document given to an inventor granting the sole rights to an invention or process. Patents have to be checked in order to validate an invention or process is an original idea. The time allotted for a patents protection is usually around 20 years after which others may use the exact same design or process with no penalty. A patent search was performed using the search service at the USPTO web site and the following patents were identified as being related to the LCFELMV2. The information supplied is the patent number and other pertinent information.

US20030037524 Electric Lawn Mower

An electric lawn mower includes a cutter blade, an electric motor disposed above the cutter blade, and a battery unit for driving the electric motor. The battery unit is positioned above the electric motor to thereby achieve weight balance of the lawn mower. This arrangement allows air to flow smoothly between the electric motor and the battery unit.

Application Number: 10/177424

Publication Date: 02/27/2003

Filing Date: 06/21/2002

What is claimed:

1. An electric lawn mower comprising: a cutter blade; a cutter housing for enclosing said cutter blade therein; an electric motor for rotating said cutter blade, said electric motor being mounted on said cutter housing; and at least one rechargeable battery unit for driving said electric motor, said battery unit being positioned above said electric motor.
2. An electric lawn mower as claimed in claim 1, wherein said cutter housing has a battery bracket attached thereto, said battery bracket including a body portion covering the sides and top of said electric motor.
3. An electric lawn mower as claimed in claim 2, wherein said battery bracket and said electric motor are secured together to the cutter housing.
4. An electric lawn mower as claimed in claim 2, wherein said battery bracket is made of metal, and has air vents formed at portions thereof where said battery unit is mounted.
5. An electric lawn mower as claimed in claim 1, wherein said electric motor includes a rotational shaft having an axis extending through said battery unit positioned above said electric motor.
6. An electric lawn mower as claimed in claim 5, wherein said cutter housing has a battery bracket attached thereto, said battery bracket including a body portion covering the sides and top of said electric motor.
7. An electric lawn mower as claimed in claim 6, wherein said battery bracket and said electric motor are secured together to the cutter housing.
8. An electric lawn mower as claimed in claim 6, wherein said battery bracket is made of metal and has air vents formed at portions thereof where said battery unit is mounted.
9. An electric lawn mower as claimed in claim 1, wherein said battery unit comprises at least one upper battery disposed above said electric motor and a front battery positioned in front of said electric motor.
10. An electric lawn mower as claimed in claim 9, wherein said cutter housing has a battery bracket attached thereto, said battery bracket including a body portion covering the sides and top of said electric motor, and an extension portion extending forward from the body portion, said body portion having said upper battery mounted thereon, said extension portion having said front battery mounted thereon, said upper battery being spaced from said front battery.

11. An electric lawn mower as claimed in claim 10, wherein said battery bracket and said electric motor are secured together to the cutter housing.

12. An electric lawn mower as claimed in claim 10, wherein said battery bracket is made of metal and has air vents formed at portions thereof where said battery unit are mounted.

US Patent 4942723 – Solar Powered Lawnmower

Publication Date: 07/24/1990

What is claimed:

1. A lawnmower comprising, in combination, an electric motor, a rechargeable battery pack, and a panel of photovoltaic cells, with said motor, said battery pack, and said photovoltaic cells electrically connected, which has said photovoltaic cells positioned in the region of the lawnmower defined by the perimeter of the handle of the lawnmower so that said photovoltaic cells are tilted at the same angle as the handle, with the angle arranged to be approximately perpendicular to the rays of the sun during periods of solar exposure to said photovoltaic cells, which has said battery pack recharged with the electricity generated by said photovoltaic cells when the lawnmower is placed in the sunlight, so that said battery pack then possesses the means to power said electric motor.

2. The lawnmower according to claim 1, which further comprises the means to employ standard AC current in order to recharge said battery pack in case of insufficient photovoltaic recharging.

PHOTOVOLTAIC MODULE-MOUNTED AC INVERTER

IPC8 Class: AH02M3335FI

USPC Class: 363 80

What is claimed:

1. An inverter for use in a photovoltaic module comprising: a DC input terminal; an AC output terminal; and a communications system for receiving and sending information through the AC output terminal.

2. The inverter of claim 1 wherein the inverter further comprises: a monitoring system for monitoring at least the voltage on the DC input terminal and the AC output terminal; a power section coupled between the DC input terminal and the AC output terminal; and a control system coupled between the monitoring system and the power section.

3. The inverter of claim 2 further comprising a charge storage element coupled to the power section.
4. The inverter of claim 2 wherein the communications system, the monitoring system, and the control system are implemented in one or more integrated circuits.
5. The inverter of claim 4 wherein the one or more integrated circuits comprise at least one active or passive component from the power section.
6. The inverter of claim 2 wherein the power section comprises a boost converter.
7. The inverter of claim 6 further comprising circuitry for measuring inductor terminal voltages in the boost converter, processing the terminals' voltages, and calculating an inductor current by dividing the processed terminal voltages by a predetermined inductance value.
8. The inverter of claim 2 wherein the power section comprises a buck converter.
9. The inverter of claim 8 further comprising circuitry for measuring inductor terminal voltages in the buck converter, processing the terminal voltages, and calculating an inductor current by dividing by the processed terminal voltages by a predetermined inductor DC resistance value.
10. The inverter of claim 2 wherein the power section further comprises a delta-sigma modulation circuit.
11. The inverter of claim 10 wherein the power section further comprises a PWM generator circuit.
12. The inverter of claim 1 further comprising a hot-swap capability.
13. The inverter of claim 12 wherein the hot-swap capability comprises circuitry for detecting disconnect conditions in at least one of the terminals and shutting down currents to the at least one terminal.
14. The inverter of claim 12 wherein the hot-swap capability comprises circuitry for testing at least one of the terminals for proper connectivity prior to enabling currents to the at least one terminal.
15. A single-inductor, bipolar-output boost converter for use in an inverter comprising: a DC input terminal; a negative DC output terminal; a positive DC output terminal; a single inductor having a first node and a second node; a first switch coupled between the DC input terminal and the first node of the inductor; a second switch coupled between ground and the second node of the inductor; a first diode having an anode coupled to the negative DC output terminal and a cathode coupled to the first node of the inductor; a second diode having an anode coupled to the second node of the inductor and a cathode coupled to the positive DC output terminal; a first capacitor coupled to the negative DC output terminal; and a second capacitor coupled to the positive DC output terminal.
16. The boost converter of claim 15 further comprising a single-cycle operating mode.
17. The boost converter of claim 15 further comprising a two-cycle operating mode.
18. A tandem bipolar-output boost converter for use in an inverter comprising: a DC input terminal; a negative DC output terminal; a positive DC output terminal; a first boost converter having a single inductor switched between the DC input terminal and ground, a first output coupled to the negative DC output terminal, and a second output coupled to the positive DC

output terminal; a second boost converter having a single inductor switched between the DC input terminal and ground, a first output coupled to the negative DC output terminal, and a second output coupled to the positive DC output terminal; a first capacitor coupled to the negative DC output terminal; and a second capacitor coupled to the positive DC output terminal.

19. The tandem converter of claim 18 further comprising a single-cycle operating mode.

20. The tandem converter of claim 18 further comprising a plurality of boost converters.

VIII. Standards

A standard is an established norm or requirement. Standards are used to make sure products are safe for consumers while also defining the quality of a company's product. A new product is tested rigorously to make sure it conforms to safety requirements of a list of standards. Standards related to photovoltaics, motors, electric safety, and appliances are listed below.

A. PV Standards

IEEE Standards

- IEEE 937 (2007) Recommended Practice for the Sizing of Lead-Acid Batteries for Photovoltaic (PV) Applications
- IEEE 1013 (2000) Recommended Practice for the Installation and Maintenance of Lead-Acid Batteries in Photovoltaic (PV) Applications
- IEEE 1361 (2003) Guide for Selection, Charging, Test and Evaluation of Lead-Acid Batteries Used in Stand-Alone Photovoltaic (PV) Systems
- IEEE 1526 (2003) Recommended Practice For Testing the Performance of Stand Alone Photovoltaic Systems
- IEEE 1561 (2007) Guide for Optimizing the Performance and Life of Lead-Acid Batteries in Remote Hybrid Power Systems
- IEEE 1562 (2007) Guide for Array and Battery Sizing in Stand-Alone Photovoltaic (PV) Systems
- IEEE 1661 (2007), Guide for Test and Evaluation of Lead-Acid Batteries Used in Photovoltaic (PV) Hybrid Power Systems
- ANSI/IEEE Std 928-1986 IEEE recommended criteria for terrestrial photovoltaic power systems.
- IEEE Std 937-2000 IEEE recommended practice for installation and maintenance of lead-acid batteries for photovoltaic systems.

- IEEE Std 1013-2000 IEEE recommended practice for sizing lead-acid batteries for photovoltaic systems.
- IEEE Std 1361-2003 IEEE guide for selection, charging, test, and evaluation of lead-acid batteries used in stand-alone photovoltaic systems.

B. ATSM Standards

- E1328-03 Standard terminology relating to photovoltaic solar energy conversion.
- E1799-02 Standard practice for visual inspections of photovoltaic modules.
- E772-87(2001) Standard terminology relating to solar energy conversion.

C. PVGAP Standards

- PVR51 Photovoltaic stand-alone systems-Design qualifications and type approval (First Edition 1997)
- PVR54 Photovoltaic (PV) stand-alone systems, with a system voltage below 50V (Third draft 2002)
- PVR55 Lead-acid batteries for solar photovoltaic energy systems (modified automotive batteries)
- PVR55A Lead acid batteries for solar photovoltaic energy systems-general requirements and methods of test for modified automotive batteries.
- PVR56 Charge controllers for photovoltaic stand-alone systems with a nominal system voltage below 50V (First edition 2000)
- PVR510 Code of practice for installation of photovoltaic systems.

D. ISO Standards

- ISO 9488:1999 Solar energy-Vocabulary

E. UL Standards

- UL 1047:2003 Standard for isolated power systems equipment, new edition.
- UL 2054.1:2003 Household and commercial batteries.
- UL 2367.1 Solid state overcurrent protectors.

F. Motor Standards

- UL 73 motor operated standards
- UL 1004 Electric Motors

G. Power Standards

- UL 62 electric power cord standards
- UL 498 Attachment Plugs and Receptacles
- UL 817 Cord Sets and Power-Supply Cords
- UL 83 thermo plastic cord standards
- UL 248-1 Low-Voltage Fuses - Part 1: General Requirements
- UL 248-14 Low-Voltage Fuses - Part 14: Supplemental Fuses
- UL 60730-2-10A Automatic Electrical Controls for Household and Similar Use; Part 2: Particular Requirements for Motor Starting Relays

H. General Appliance Standards

- UL 94 flammability of plastic materials for parts in devices and appliances
- UL 510 Polyvinyl Chloride, Polyethylene, and Rubber Insulating Tape
- UL 969 Marking and Labeling Systems
- UL 1439 Tests for Sharpness of Edges on Equipment

I. IEC Standards

- IEC 60730-2-10 Ed. 2.0 b:2006 Automatic electrical controls for household and similar use - Part 2-10: Particular

- IEC 62093 Ed. 1.0 b:2005 Balance-of-system components for photovoltaic systems - Design qualification natural environments

References

- Kamp, Kraig, David Sharpe, and Jamin Williams. Low Carbon Footprint Electric Lawn Mower. Electrical Engineering, Bradley University.
- Chuck. "1 Hp Scott Motor." V is for Voltage Forums (R).
<<http://visforvoltage.org/forum/forums/1927>>.
- "Lawnmower Safety Standards." 03 Dec. 2004. LSU AgCenter.
<http://text.lsuagcenter.com/en/lawn_garden/commercial_horticulture/equipment/Mowing/Lawnmower+Safety+Standards.htm>
- "Normas ANSI Standards." ANSI Standards.
<http://www.ingefix.cl/certificados/html_ansi.htm>.
- "NPC-Black Max." NPC Robotics. 8 Jan. 2009.
<<http://www.npcrobotics.com/products/viewprod.asp?prod=33&cat=20&mode=gfx>>
- Patent Searching and Inventing Resources. 02 Feb. 2009
<<http://www.freepatentsonline.com>>.
- "SCC21 Published Activities and Projects." 2008. IEEE.
<<http://grouper.ieee.org/groups/scc21/published.html>>.
- "U.S. Solar Radiation Resource Maps." National Renewable Energy Laboratory Resource Assessment Program. 15 Jan. 2009.
<http://rredc.nrel.gov/solar/old_data/nsrdb/redbook/atlas/Table.html>.

Appendix

The company that sold the Motor Scott 1 HP motor did not provide performance curves and we found the performance curve at <http://visforvoltage.org/forum/forums/1927>. This performance curve was confirmed because the Motor Scott 1 HP is being rebranded by NPC Robotics as the NPC-4200 motor and NPC Robotics provided dyno test data for the NPC-4200 motor

Motor Scott Performance Curves

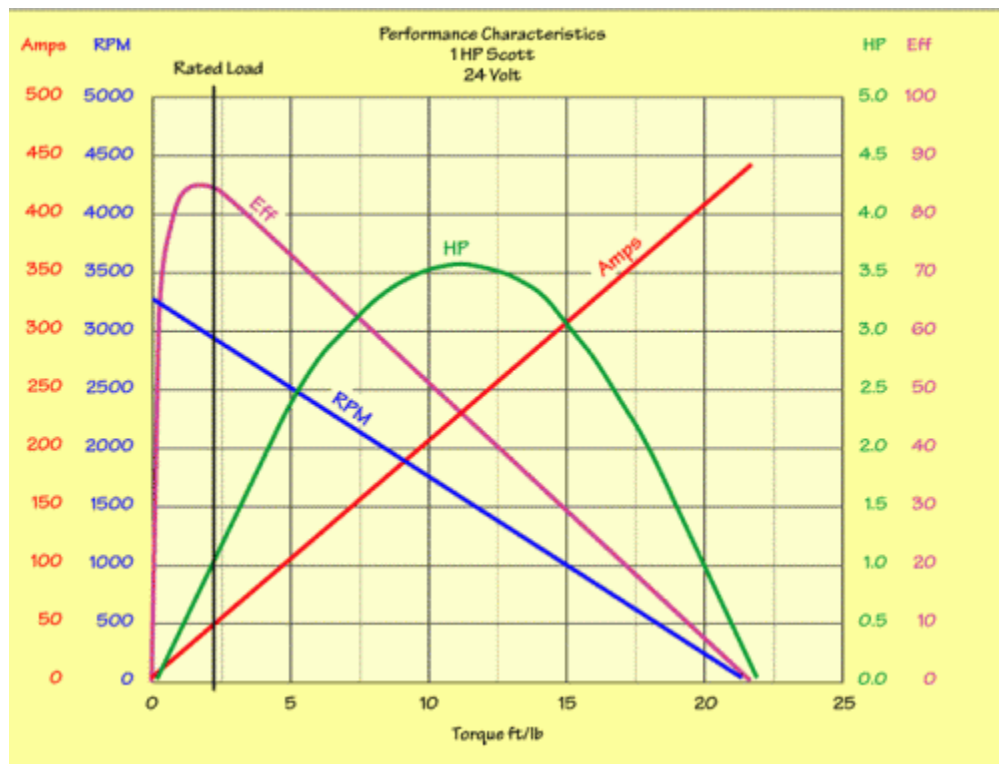


Figure 23 – Motor Scott 1 HP performance curves at 24 volts

NPC-4200 Performance Curves

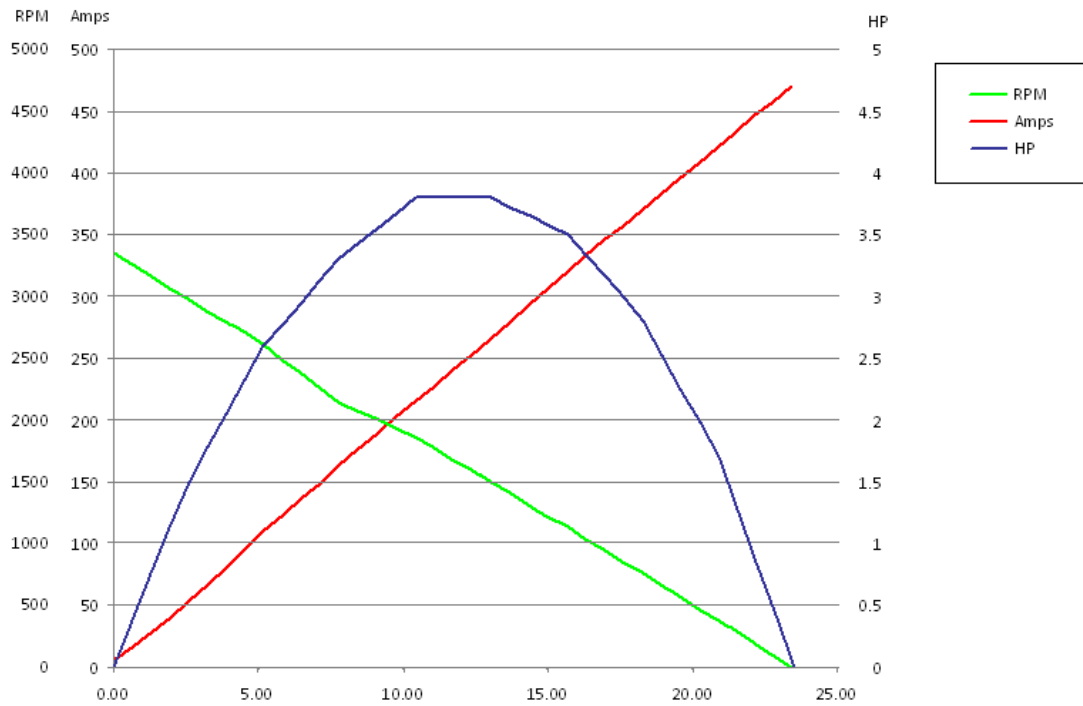


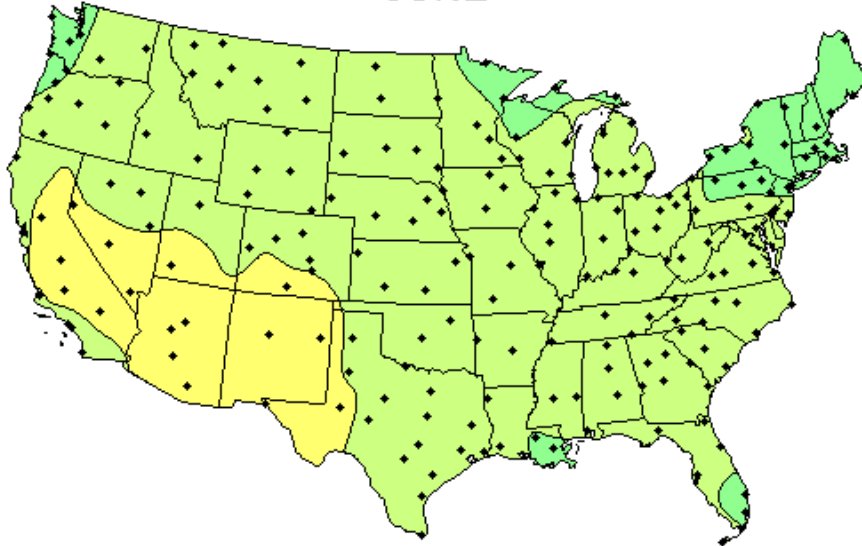
Figure 24 – NPC-4200 performance curves based on dyno test data²

² NPC Robotics - <http://www.nprobotics.com/products/viewprod.asp?prod=33&cat=20&mode=gfx>

Isolation Data – June

Minimum Daily Solar Radiation Per Month

JUNE



Flat Plate Tilted South at Latitude + 15 Degrees

This map shows the general trends in the amount of solar radiation received in the United States and its territories. It is a spatial interpolation of solar radiation values derived from the 1961-1990 National Solar Radiation Data Base (NSRDB). The dots on the map represent the 239 sites of the NSRDB.

Maps of average values are produced by averaging all 30 years of data for each site. Maps of maximum and minimum values are composites of specific months and years for which each site achieved its maximum or minimum amounts of solar radiation.

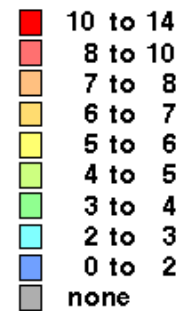
Though useful for identifying general trends, this map should be used with caution for site-specific resource evaluations because variations in solar radiation not reflected in the maps can exist, introducing uncertainty into resource estimates.

Maps are not drawn to scale.



National Renewable Energy Laboratory
Resource Assessment Program

kWh/m²/day



FP15D06-292

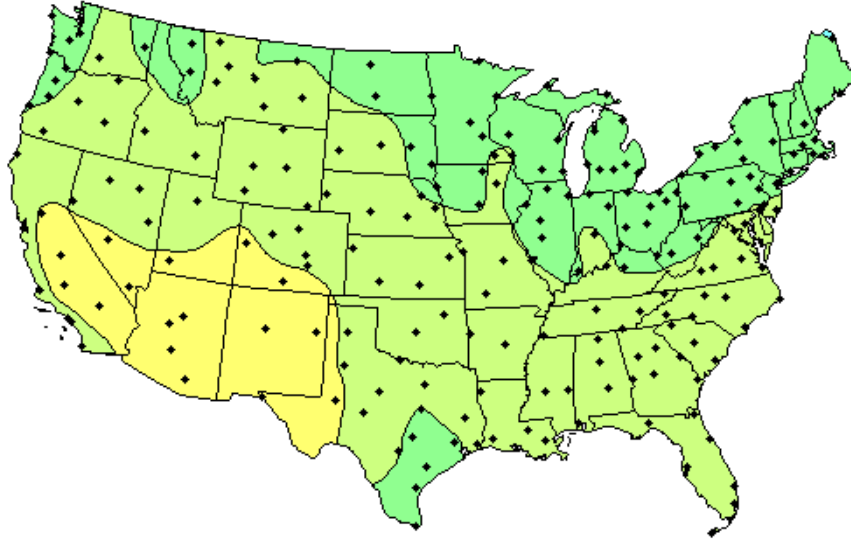
Figure 25 – Isolation Data for June, Minimum Daily Solar Radiation³

³ National Renewable Energy Laboratory Resource Assessment Program,
http://redc.nrel.gov/solar/old_data/nsrdb/redbook/atlas/Table.html

Isolation Data – May

Minimum Daily Solar Radiation Per Month

MAY



Flat Plate Tilted South at Latitude + 15 Degrees

This map shows the general trends in the amount of solar radiation received in the United States and its territories. It is a spatial interpolation of solar radiation values derived from the 1961-1990 National Solar Radiation Data Base (NSRDB). The dots on the map represent the 239 sites of the NSRDB.

Maps of average values are produced by averaging all 30 years of data for each site. Maps of maximum and minimum values are composites of specific months and years for which each site achieved its maximum or minimum amounts of solar radiation.

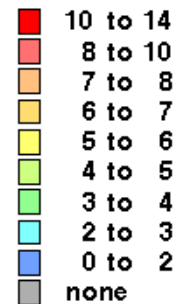
Though useful for identifying general trends, this map should be used with caution for site-specific resource evaluations because variations in solar radiation not reflected in the maps can exist, introducing uncertainty into resource estimates.

Maps are not drawn to scale.



National Renewable Energy Laboratory
Resource Assessment Program

kWh/m²/day



FP15D06-291

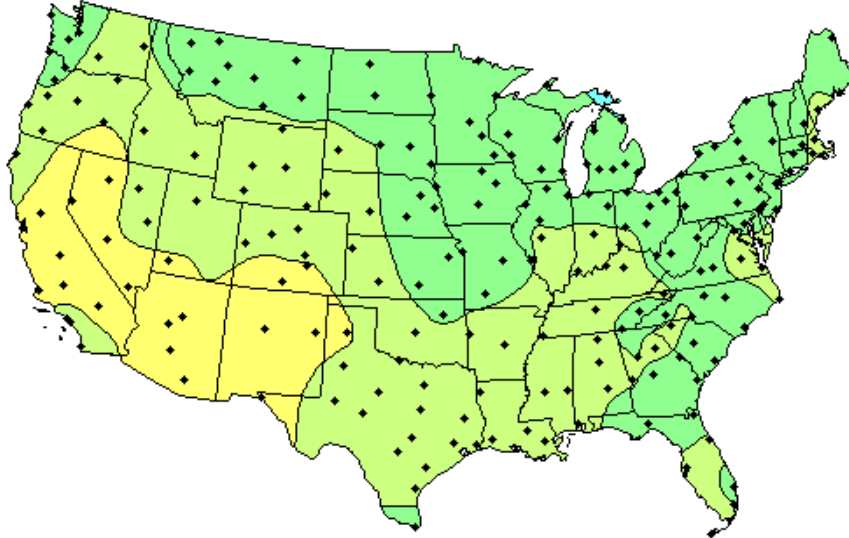
Figure 26 – Isolation Data for May, Minimum Daily Solar Radiation⁴

⁴ National Renewable Energy Laboratory Resource Assessment Program, http://redc.nrel.gov/solar/old_data/nsrdb/redbook/atlas/Table.html

Isolation Data – September

Minimum Daily Solar Radiation Per Month

SEPTEMBER



Flat Plate Tilted South at Latitude + 15 Degrees

This map shows the general trends in the amount of solar radiation received in the United States and its territories. It is a spatial interpolation of solar radiation values derived from the 1961-1990 National Solar Radiation Data Base (NSRDB). The dots on the map represent the 239 sites of the NSRDB.

Maps of average values are produced by averaging all 30 years of data for each site. Maps of maximum and minimum values are composites of specific months and years for which each site achieved its maximum or minimum amounts of solar radiation.

Though useful for identifying general trends, this map should be used with caution for site-specific resource evaluations because variations in solar radiation not reflected in the maps can exist, introducing uncertainty into resource estimates.

Maps are not drawn to scale.



National Renewable Energy Laboratory
Resource Assessment Program

kWh/m²/day



FP15D09-296

Figure 27 – Isolation Data for September, Minimum Daily Solar Radiation⁵

⁵ National Renewable Energy Laboratory Resource Assessment Program,
http://rredc.nrel.gov/solar/old_data/nsrdb/redbook/atlas/Table.html